

We are IntechOpen, the world's leading publisher of Open Access books Built by scientists, for scientists

6,900

Open access books available

186,000

International authors and editors

200M

Downloads

Our authors are among the

154

Countries delivered to

TOP 1%

most cited scientists

12.2%

Contributors from top 500 universities



WEB OF SCIENCE™

Selection of our books indexed in the Book Citation Index
in Web of Science™ Core Collection (BKCI)

Interested in publishing with us?
Contact book.department@intechopen.com

Numbers displayed above are based on latest data collected.
For more information visit www.intechopen.com



Phase Transitions and Structure of Liquid Crystalline Cellulose Ether Solutions in a Magnetic Field and in Its Absence

Sergey Vshivkov and Elena Rusinova

Abstract

The results of research studies of a magnetic field effect on structure and phase transitions of liquid crystalline polymer systems are described. Influence of intensity of the magnetic field, molecular weight, and concentration of polymers in solutions on the phase diagrams is analyzed. The dependences of boundary curves on the chemical structure of polymers and solvents are discussed. Results of theoretical researches of the magnetic field effect on the diamagnetic macromolecule orientation in solutions are described. The shift of boundary curves of liquid crystalline cellulose derivative systems is compared with the energy of magnetic field stored by solutions.

Keywords: liquid crystalline polymer systems, magnetic field, structure, phase transitions

1. Introduction

1.1 Liquid crystalline state of matter

Matter can exist in the following phase states: crystalline, amorphous (liquid), gaseous, and liquid crystalline. The substances in the different phase states exhibit the different spatial arrangements of structural elements (molecules, atoms, ions).

The crystalline phase state is characterized by a three-dimensional long-range order in arrangement of atoms or molecules. Long-range orientational order is an order observed over distances hundreds and thousands of times larger than the size of the molecules and can exist in one, two, or three dimensions.

The amorphous phase state (liquid phase state) is characterized by a short-range orientational order, i.e., an order observed over distances commensurate with molecular size. In the vicinity of any given molecule, its neighbors can be ordered but at a small distance from the molecule. The amorphous phase state is attributed to all liquids (excluding mercury) as well as glass and other solid noncrystalline substances.

In a gaseous phase state, there is no order in the spatial arrangement of structural elements.

The term “liquid crystal” is a contradiction in itself. The crystals are considered to be anisotropic solids showing usually very low deformations even under high mechanical stress. On the other hand, the fluids are able to flow, and they exhibit isotropic optical properties. Meanwhile, over a hundred years ago, it was found [1] that some organic substances in melt, that is they are able to flow, exhibit anisotropic optical properties (birefringence). Such a substance was first described in 1888 by F. Reinitzer [2], Professor of the Botanic School of Graz University of Technology (Austria). He examined the physiological activity of cholesterol, the chemical formula for which had not yet been determined. In the course of his studies, F. Reinitzer synthesized cholesterol derivatives and determined their melting temperatures. He found that cholesteryl benzoate under melting at 145.5°C turned into a cloudy liquid and after further heating, turned into transparent melt at 178.5°C. The refractive indices of the cloudy melt measured in two perpendicular directions were different, which proved its anisotropic properties. Therefore, F. Reinitzer assumed that the turbid melt included two substances. F. Reinitzer tried to separate the substances, but he could not, and so he sent a cholesteryl benzoate sample for examination to physicist, Prof. Lehmann, who lived in Dresden. Prof. Lehmann examined the sample with a polarizing microscope and concluded that the turbid melt did not comprise two different liquids but presented a single liquid crystal [3]. Thus, it was Lehmann who introduced the term “liquid crystal.” In 1890, he discovered liquid crystals of ammonium oleate, para-azoxyanisole, and para-azoxyphenetole.

The nature of a liquid crystalline (LC) phase state is as follows: some substances, as soon as they reach the temperature at which the three-dimensional lattice disintegrates, do not exhibit the direct transition to isotropic liquid but hold intermolecular order. In LC systems the order is not three-dimensional but, according to Gray, one- or two-dimensional, i.e., the regularity is partially destroyed, but the long-range orientational order always remains in one or two directions. Such behavior determines, on the one hand, an essential fluidity (ability for irreversible deformation) and, on the other hand, a demonstration of anisotropic physical properties in contrast to liquids possessing a short-range order.

Further detailed study of LC substances revealed that the crystal-liquid crystalline transition and consequent liquid crystalline-liquid (amorphous) transition are phase transitions of the first order and that the liquid crystals are in a special phase state, which is neither conventional crystalline nor amorphous phase state.

Liquid crystalline state is a thermodynamically stable phase state at which the matter exhibits the stable anisotropic physical properties of crystalline solids and the fluidity typical for liquids [4].

As liquid crystal exists between crystalline and amorphous phase states, it is called “mesomorphic phase” (“mesos” in Greek means middle, intermediate). The term “mesomorphic phase” or “mesophase” was introduced by Friedel in 1922.

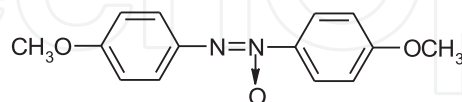
The majority of liquid crystals have an enantiotropic mesophase, i.e., they appear upon both the melting of a crystalline solid and the cooling of a melt. However, some liquid crystals possess a monotropic mesophase appearing only upon cooling [5].

The main cause of matter transition to a liquid crystalline phase state, as soon as the melting point is achieved, is the asymmetric molecule structure. All matters demonstrating the transition to mesophase consist of the elongated molecules. At T_{melt} , the intermolecular forces of lattice are not enough to hold molecules in the fixed position, and the three-dimensional lattice breaks down. On the other hand, the molecule anisotropy is an important factor of the preservation of a certain degree of intermolecular order. An additional kinetic energy is required to break this relative order too. So, a so-called step-by-step transition is observed from true

crystal order to a random amorphous phase state. Each of these “steps” is characterized by strictly defined latent heat of transition. As a rule, the latent heat of the liquid crystalline-amorphous state transition is not high [5]. The basic change occurs at the initial disintegration of the three-dimensional crystalline lattice.

As mentioned above, the liquid crystalline systems demonstrate one- and two-dimensional orders [1]. A one-dimensional order of molecules means only a long-range orientation order along the molecule axes (**Figure 1**).

The gravity center of individual molecules is not coordinated relative to each other, and molecules can have a casual azimuthal deviation from the main axis. Such a structure is called nematic. Nematic systems are the first type of liquid crystal. For example, *n*-asocsianisol (PAA) [5]:



The patterns of so-called cholesteric systems are more ordered in comparison to nematic liquid crystals (**Figure 2**).

Their structure is a combination of parallel nematic layers where the direction of axes of molecules within each following layer is turned on a certain angle concerning the direction of molecule axes in the previous layer. Thus, a helix appears with a pitch that can be of several hundreds of nanometers. The equidistant arrangement of parallel layers and constant helix pitch allow the formal classification of this type of structure as two-dimensional; however, the molecule orientation

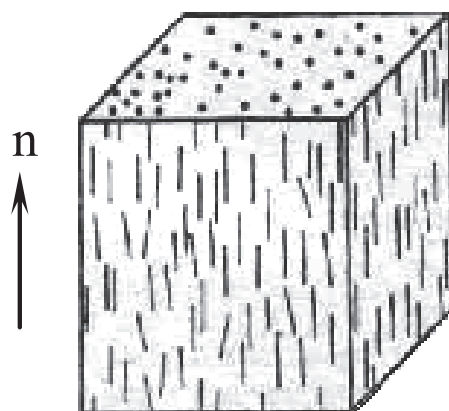


Figure 1.
Nematic mesophase [5].

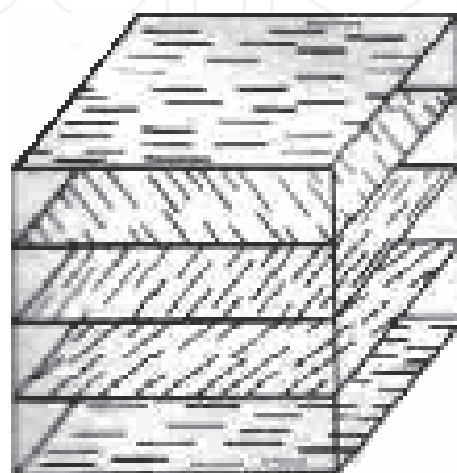
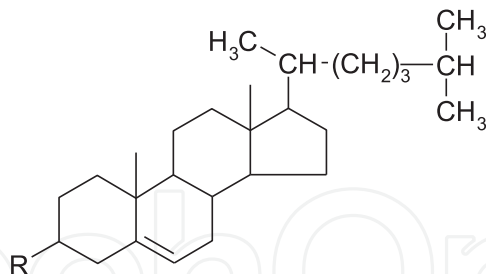
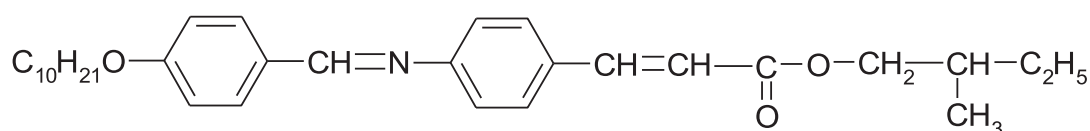


Figure 2.
Cholesteric mesophase [5].

within the layers is of a nematic nature due to which the cholesteric liquid crystals are sometimes referred to as a variant of the nematic phase. The cholesteric liquid crystals are so called because they are the complex esters of cholesterol, mainly:



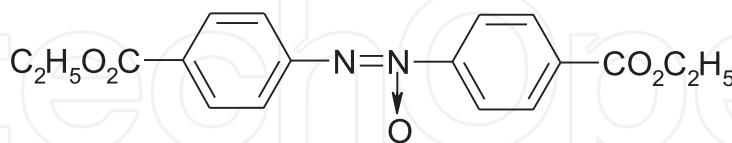
where R is the residue of relevant acid. But the complex esters of cholesterol are not the only representatives of cholesteric structure. A cholesteric mesophase is characteristic to other compounds, for example, 4'-(4-methoxybenzyl idenamin) aril cinnamate over a range of temperatures from 82 to 102°C [5]:



All such compounds contain asymmetric (chiral) atoms of carbon. Chiral properties give rise to the formation of a cholesteric mesophase. If the mesogenic compound is able to form a nematic phase and its molecules are chiral, then a cholesteric mesophase appears. This is proved by the fact that an addition to the nematic of a small amount of the cholesteric or chiral compound, which is not mesogenic, transfers the latter to the cholesteric. It should be noted that when changing the external conditions, the helix pitch may alter by discrete quantities up to infinity. Under such conditions, the cholesteric liquid crystal-nematic liquid crystalline transition is observed.

The smectic liquid crystals are the most ordered. They represent two-dimensional liquid crystals: the centers of molecule mass are located in layers, but the director n of each layer is no longer aligned along the layer surface but is tilted at a certain angle to it (**Figure 3**).

These liquid crystals are usually referred to smectic A, which is the most commonly found among smectic liquid crystals. The typical example of A smectic is ethyl ester of *n*-nitrooxybenzoic acid (ENB) [5]:



within temperatures from 114 to 120°C.

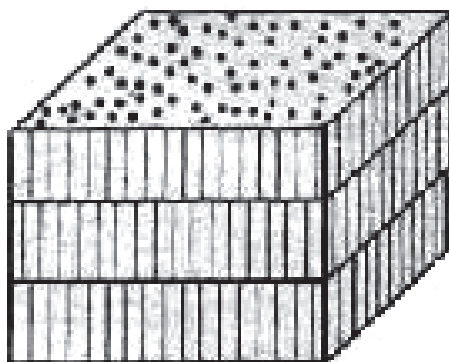
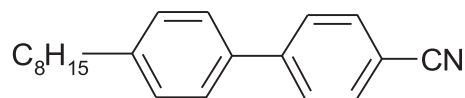


Figure 3.
Smectic A mesophase [5].

The thickness of layers is usually equal to the length of molecules of mesogen and the majority of the smectics exhibits such property. But for some smectics, the layer thickness is less than the molecular length or exceeds it. This is determined by the peculiarities of molecular structure.

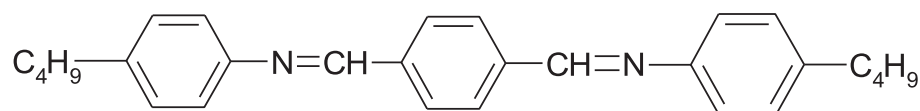
For example, the layer thickness of 4-cyano-4'-*n*-octylbiphenyl:



exceeds the molecule length by 1.4 times. In this case, a double-layered structure seems to exist and as such molecules within one layer enter the gaps between the molecules of the other layer.

The smectics with non-ordered layers are called *smectic C* or tilted smectics (**Figure 4**).

They are commonly classified into smectic *C* with a small ($\omega < 30^\circ$) and big ($\omega \approx 45^\circ$) tilt angle of the director to the normal layer. Upon heating the smectic *C* with a small tilt angle transfers into smectic *A*. However, some compounds, such as terephthal-bis-4-*n*-butylaniline (TBBA):



within the temperatures from 114.1 to 172.5°C, where the smectic *C* phase exists, exhibit a tilt angle ω depending on temperature and upon heating tilt angles become zero.

In such structures, the director processes around the cone from one layer to the next. Such a structure is similar to cholesteric.

Liquid crystals appearing upon cooling or heating by individual matters are called thermotropic. Liquid crystals resulting from the dissolution of matters are called lyotropic.

In [4], the mesogenic compounds are classified into the following groups based on their chemical structure:

1. aromatic compounds without bridge groups;
2. heteroaromatic compounds without bridge groups;
3. aromatic compounds with one bridge group;
4. aromatic compounds with several similar bridge groups;

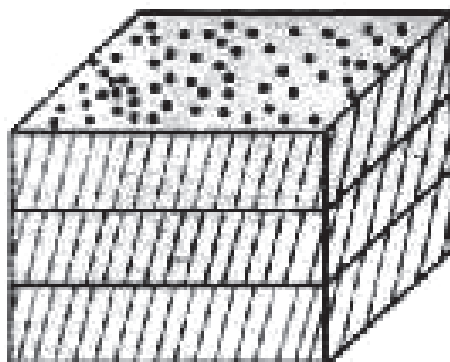
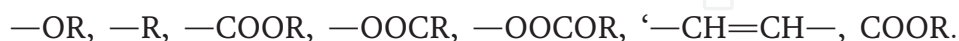


Figure 4.
Smectic C mesophase.

5. aromatic compounds with different bridge groups;
6. stilbene, amides of carbon acid, derivatives of hydrazine and glyoxal;
7. aromatic carbon acids;
8. carbonic acid salts and ammonium salts;
9. alicyclic and aliphatic compounds.

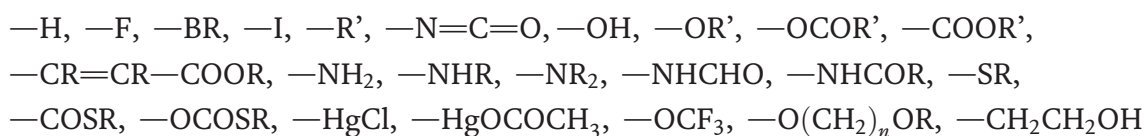
Following the above classification, the various chemical fragments used in synthesis of mesogenic compounds are listed below (*R* is the n-alkyl; *R'* is the branched or unsaturated alkyl): most often used:



often used:



seldom used:



If one and the same substance has both nematic and smectic phases, the temperature of a smectic phase is always lower than the temperature of a nematic phase. Upon heating or cooling of the matter with the symmetrical molecules, the phase transitions from crystalline solids (CS) to isotropic liquids (IL) occur according to the scheme:



Transition temperatures are repeatable and reversible in case of enantiotropic transitions. Matters with optically active molecules exhibit the phase transitions according to the following scheme:



1.2 Specific behavior of polymer liquid crystalline state

The specifics of polymers include both nonequilibrium states and manifestations of features, typical of an LC state, when the polymer is in an amorphous but not in a mesomorphous state. The majority of flexible chain polymers are subjected to orientational stretching during their manufacturing. If this is followed by a glass transition of the polymer system, the orientational order remains practically infinitely long. The resulting structure is nonequilibrium since after prolonged heating and slow cooling down to the original temperature, the system exhibits a clear tendency to disorder through weakening anisotropic properties [1].

The difference in phase transitions between the low-molecular matters and polymers should be assumed not in the special thermodynamic behavior of mesophase but rather in the kinetics of these transformations. The higher speed of phase transitions in low-molecular systems is quite clear as well as the lower speed of such

transformations in polymers. These general properties of polymer systems and transitions to LC state and especially the liquid crystalline-crystalline solid transition, such as direct amorphous-crystalline solid transition, can be accompanied by such long periods of induction that they are not comparable to internal observation.

It should be noted that the rigid-chain polymers that most probably form the liquid crystals due to the high geometric anisotropy of molecules melt at temperatures higher than the temperatures of their intensive thermal destruction. Thus, polymers (with few exceptions) are unlikely to produce thermotropic LC systems. Apparently, this allowed Ph.H. Geil to consider the formation of only lyotropic liquid crystals though at present, thermotropic high-molecular LC systems are also known; for example, the melt of polypropylene, hydroxypropyl cellulose, as well as system based on block copolymers [5–8].

The appearance of a mesophase in polymer systems is caused by the following [1]:

1. The ordering caused by the interaction of rather long side groups (side chains) in polymers.
2. The ordering caused by the interaction of homogeneous sequences (blocks) in block copolymers.
3. The ordering caused by the molecule rigidity. The distribution of rigid macromolecules in melts and solutions cannot be random. The polymer systems with rigid macromolecules exhibit a spontaneous transition to ordered states, which do not achieve a three-dimensional order; they are limited by the one- or two-dimensional order.

The degree of orientational order is mainly determined by the flexibility of macromolecules, which is measured by Khun’s segment *A*. The values of Khun’s

Polymer	<i>A</i> , nm	<i>M</i> × 10 ^{−3}	<i>Q</i>
Poly-γ-benzyl-L-glutamate	240	33–330	0.88–0.38
Polybutyl isocyanate	100	15–150	0.76–0.19
Poly-hlorohexyl isocyanate	48	24–240	0.57–0.10
Poly-para-benzamide	110	5.5–55	0.45–0.18
Poly-para-phenyleneterephthalamide	65	5.5–55	0.46–0.13
Poly-para-amide-hydrazide	45	5.5–55	0.39–0.09
Poly-meta-phenylenisophthalamide	5	5.9–59	0.1–0.01
DNA	90	58.3–583	0.72–0.17
Double-chain polyphenylensiloxan	20	31–310	0.34–0.04
Cellulose nitrate	23	17.3–173	0.37–0.05
Ethyl cellulose	20	14–140	0.33–0.05
Cellulose phenylcarbanilate	16	23–230	0.28–0.04
Polystyrene	2	12–120	0.04–0.004
Polyethylene	2	3.3–33	0.04–0.004
Polymethylmethacrylate	2	12–120	0.04–0.004

Table 1.
Values of *Q* and *A* for polymers of various molecular weights [6].

segments and the parameters of the intermolecular orientational order Q of different polymers are given in **Table 1**.

Table 1 shows that with an increase in the flexibility of macromolecules (reduction of Khun's segment size) and in the polymer molecular mass, the value of the intermolecular orientation order decreases. It is important to emphasize that the transitions of the rigid-chain polymers into the LC state usually occur in solutions rather than in melts.

1.3 Effect of magnetic field on liquid crystalline systems

Low-molecular-mass liquid crystals exhibit a good orientation in the magnetic and electric fields. In general, this is associated with the anisotropy of diamagnetic susceptibility $\Delta\chi$ or dielectric permittivity $\Delta\epsilon$ parallel and perpendicular to the long axis of molecules. The molecules of LC substances are ordered so that the direction with the higher values of χ (or ϵ) is parallel to a vector of field intensity [1]. However, the behavior of polymer LC systems in the force fields has not been studied enough.

The theory of the interaction of diamagnetic macromolecules with a magnetic field is in the development stage [9–13]. If such a macromolecule is placed in a magnetic field, then the force acting on it will cause it to rotate. This is due to the magnetic anisotropy of the molecule, depending on the magnetic anisotropy of chemical bonds. In these systems, an orientation of chains proceeds cooperatively. The magnetic field leads to the orientation of macromolecular domains in a certain predominant direction that depends on the sign of diamagnetic susceptibility anisotropy $\Delta\chi^M$ for this polymer. Domains are taken to mean the anisotropic associates of macromolecules. The diamagnetic moment appearing at the domain can be written as [9, 10]:

$$\mu = \Delta\chi^M B^2 V \sin 2\xi / 2\mu_0 \quad (1)$$

where V is domain volume, μ_0 is a magnetic constant of vacuum, B is a vector of magnetic induction, ξ is an angle between the direction B and the domain axis.

Interaction of external magnetic field with the domain having the magnetic moment μ increases energy of magnetic field by value of E_{mag} . Orientation is observed when E_{mag} exceeds the amount of thermal energy. In this case, the following conditions must be met [9, 11]: first, the particle must be anisodiametric; secondly, the volume of the particle must be greater than the critical value.

$$V_{\text{crit}} = 2kT\mu_0 / B^2 I \Delta\chi I, \quad (2)$$

where μ_0 is the magnetic constant of vacuum, B is the vector of magnetic induction, $\Delta\chi$ is the anisotropy of diamagnetic susceptibility, k is the Boltzmann constant, and T is the absolute temperature;

third, the medium should be low viscosity.

The influence of the magnetic field on the liquid crystals was studied by Mayer [14] and de Gennes [15]. They examined the behavior of a cholesteric liquid crystal under magnetic field and found that at the critical intensity H_c of magnetic field, the complete transition to the nematic LC structure is observed. And

$$H_c = \frac{\pi^2}{2} \left(\frac{K_{22}}{\Delta\chi_m} \right)^{1/2} \frac{1}{p_0} \quad (3)$$

where p_0 is the pitch of the cholesteric helix before exposure of the magnetic field, $\Delta\chi_m$ is the anisotropy of magnetic susceptibility of the liquid crystal, K_{22} is the module of the resilience of cholesteric mesophase. This equation takes into account the anisotropy $\Delta\chi$ of one molecule. The theory predicts the slow increase in the pitch of the cholesteric helix at the small intensity of the magnetic field and the exponential increase in the pitch of the cholesteric helix near the critical intensity of the magnetic field.

The theory has been checked for the lyotropic PBG liquid crystals in a number of solvents [16, 17]. According to Miller et al. [18], the molecules of liquid crystals are oriented parallel to the magnetic field lines. This orientation is related to the anisotropy of the magnetic susceptibility of molecules, which in turn is associated with the anisotropy of their structure. The effect of a magnetic field on the properties of polymer systems is discussed in [19–28].

Since 2006, researchers of the Chair of Macromolecular Compounds, Ural State University investigate the effect of magnetic field on the phase transitions, structure and rheological properties of liquid crystalline solutions of cellulose ethers [12, 13, 29–36].

2. Phase diagrams of solutions of rigid-chain polymers

A qualitative approach to examination of the solutions of rigid-chain polymers with rigid rod-shaped molecules reveals that an independent position (a random orientation) of each molecule is possible only in relatively diluted solutions. As the number of macromolecules in the given volume of solution increases, the probability of the random orientation of the rigid rod-shaped molecules decreases, and as soon as the polymer concentration reaches a certain critical value, the further increase in the number of molecules in the volume proves to be impossible without the relative ordering of part of them. Thus, it should be followed by separation in two phases, one of which exhibits ordered macromolecules and the other that ensures that molecules are randomly oriented relative to each other. As the concentration of polymer continues to increase, the share of the ordered phase grows, and eventually the system becomes one-phased again while all macromolecules are relatively ordered [1, 14, 29–37].

The first molecular theory of nematic ordering was offered by Onsager in 1949 [38] for a solution of long rigid cylindrical rod-shaped molecules of length L and diameter ($L \gg d$). Such a system is a simulation of the solution of extremely rigid-chain macromolecules with flexibility too small to be noticed along the L length. Onsager examined a case of an athermic solution where only repulsive forces exist between rod-shaped molecules due to their relative impermeability and the liquid crystalline ordering is caused by the steric factors. He revealed that:

1. orientation order in solutions of long rigid rod-shaped molecules is a phase transition of the first order occurring at a low concentration of rod-shaped molecules in solution ($\varphi_2 \sim d/L$);
2. at $\varphi_2 < \varphi_{2i}$, the solution is isotropic; at $\varphi_2 > \varphi_{2a}$, it is anisotropic; and at $\varphi_{2i} < \varphi_2 < \varphi_{2a}$, the solution separates into isotropic and anisotropic phases, where

$$\varphi_{2i} = 3.34(d/L); \varphi_{2a} = 4.49(d/L) \quad (4)$$

3. order parameter $Q = \langle 3 \cos^2 \theta - 1 \rangle / 2$ in the point of LC phase appearance (i.e. at $\varphi_2 = \varphi_{2a}$) is equal to $Q = 0.84$.

Another approach to solving the problem of LC ordering in the solution of rigid rod-shaped molecules was developed by Flory in 1956 based on the lattice theory of solutions [39]. He introduced the following equation to describe free energy change:

$$\Delta G_{sm}/(RT) = n_1 \ln \varphi_1 + n_2 \ln \varphi_2 - (n_1 + y n_2) \ln [1 - \varphi_2(1 - y/x)] - n_2 [\ln(xy_2) - y + 1] + \chi_1 x n_2 \varphi_1, \quad (5)$$

where φ_1 and φ_2 are the volume fractions of solvent and polymer, respectively; n_1 and n_2 are the quantity of molecules of solvent and polymer, respectively; χ_1 is the Flory-Huggins interaction parameter; y is the parameter of macromolecule disorientation; x is the degree of molecule asymmetry ($x = L/d$, L is the length of a molecule, d is the diameter of a molecule).

As a result of the minimization of free energy of the system ΔG_{sm} , it was revealed [39] that critical volume fraction of polymer φ_2^* , at which LC phase appears at $x > 10$ accurate within 2%, is equal to:

$$\varphi_2^* \cong \frac{8}{x} \left(1 - \frac{2}{x}\right) \quad (6)$$

Based on Flory's theory, a phase diagram of rigid-chain polymer solution was constructed.

The limits of the separation region in the case of athermal solution at $x \geq 200$ were described by Flory as follows:

$$\varphi_i = 8/x, \quad \varphi_a = 12.5/x. \quad (7)$$

Flory's lattice theory, despite its artificial character, can be successfully applied to the solving of a number of certain problems when other approaches require too complicated computations. The examples of phase diagrams based on experimental results are given below.

The phase diagram of PBG-DMF systems, experimentally found by Miller et al. [40] by methods of polarizing microscopy, viscometry, and nuclear magnetic resonance (NMR), exhibits the rather close agreement with Flory's theoretical diagram as shown in **Figure 5**. The experimental diagram represents a dashed region having been defined with low accuracy (**Figure 6**) [40]. According to Flory's calculations, this region testifies to the coexistence of two anisotropic phases.

In the diagram of poly-carbobenzoxyllysine-DMF system (**Figure 7**) [40], the narrow region of the coexistence of isotropic and anisotropic phases is observed, which becomes broader only at very low temperature values. Though the rather high freezing point of DMF prevents obtaining experimental values in the region where the compositions of coexisting phases approach pure solvent and pure polymer correspondingly, the tendency toward transition to this area is quite obvious.

The diagram in **Figure 8** was obtained by Iovleba et al. [41]. One can see that it represents the part of the theoretical diagram associated with the narrow region of the coexistence of isotropic and anisotropic phases.

The phase diagrams were constructed for the following systems: PBA-DMAC [42], PBG-benzyl alcohol [43], PPTA (poly-p-phenylene terephthalamid)-H₂SO₄-water [44], PBG-m-cresol [45], copolymer of p-phenylenediamine with terephthalic acid-H₂SO₄, and copolymer of p-phenylene-diamine with 4,4'-(diphenyl dicarbonic) acid-H₂SO₄ [46], PBG-dichlorine acetic acid [47].

While examining polymer LC systems, one cannot but refer to the studies dedicated to exploring the LC states of cellulose and its derivatives [48]. Cellulose is one of the most widespread natural polymers used intensively in various industries. The liquid crystalline state in solutions and melts of several cellulose derivatives was

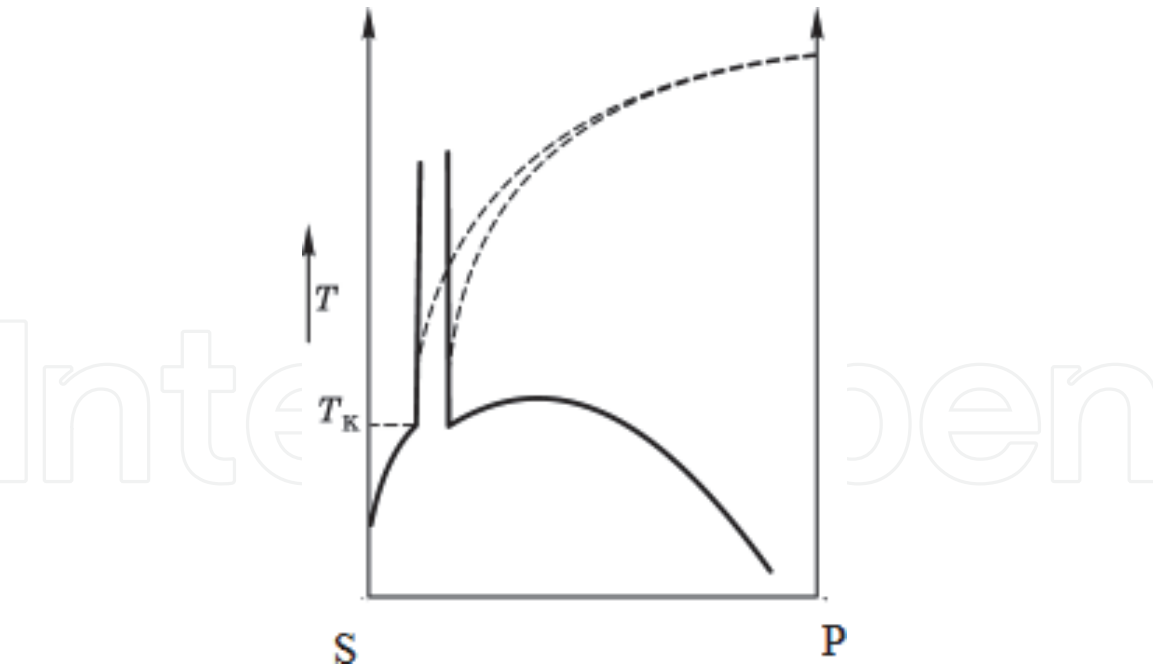


Figure 5.
Phase diagram for a system of rigid-chain polymer-solvent based on Flory's theory (dashed line shows a deviation from the theoretical behavior corresponding to the temperature effect on the phase composition).

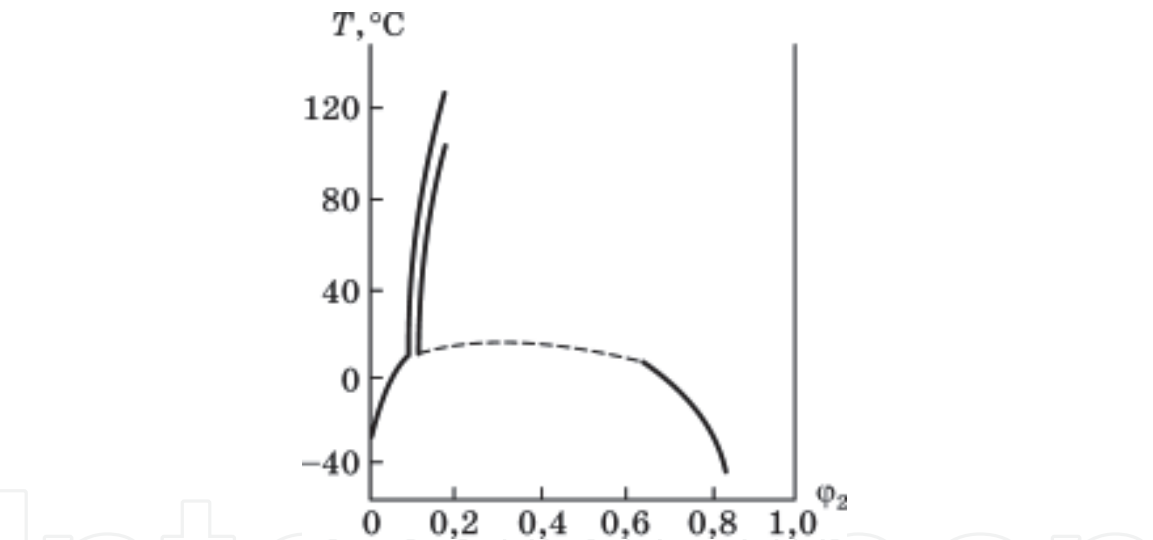


Figure 6.
Phase diagram of poly- γ -benzyl-L-glutamate (PBG)-dimethylformamide (DMF) system [40].

discovered in the 1980s. A number of studies of molecular structure of cellulose and its derivatives revealed that they have a helical conformation in the ordered regions being stabilized by intermolecular hydrogen bonds. If during the dilution of the aforesaid polymers the intermolecular H-bonds remain, the molecules continue to be rigid-chained and therefore are able to produce the ordered structures and form a mesophase. If during the dilution the intermolecular H-bonds are disrupted, the macromolecules become flexible and as a result cease to be ordered. Thus, to maintain the LC solution of cellulose and its derivatives, so-called chiral forming solvents are used to disrupt only the intermolecular H-bonds (DMF, DMAC, 1,4-dioxane, chlorinated hydrocarbons) [48].

Figures 9 and 10 show the phase diagrams of solutions of cellulose derivatives.

Systematic studies of liquid crystalline phase transitions in solutions of cellulose esters were carried out at the polymer chair of Ural Federal University [12, 13, 29–36].

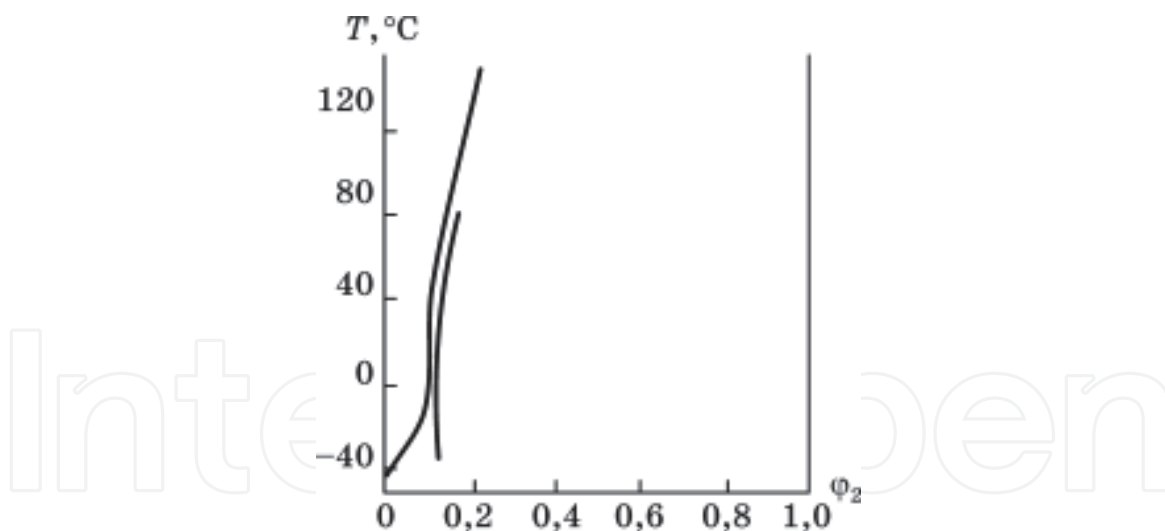


Figure 7.
Phase diagram of polycarbobenzoxylysine-DMF system [40].

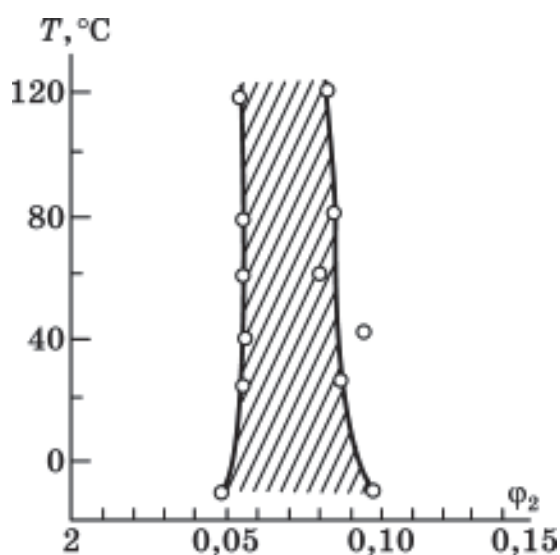


Figure 8.
Phase diagram of poly-*p*-benzamid (PBA)-dimethylacetamide (DMAc) systems (+3% mass. LiCl) [41].

The objects of this study were hydroxypropyl cellulose (HPC) of the Klucel-JF trademark (Hercules, United States); cyanoethyl cellulose (CEC), cyanoethylnitrocellulose (CENC), cyanoethyl, hydroxyethyl cellulose (CEHEC), and methyl cellulose (MC) (Institute of Macromolecular Compounds, Russian Academy of Sciences, Russia); and hydroxyethyl cellulose (HEC) and ethyl cellulose (EC) (Hercules-Aqualon and ACROS–USA). Their characteristics are presented in Table 2.

2.1 Effect of polymer molecular mass on phase LC transitions in cellulose ether-solvent systems

According to [39], the critical volume fraction of a polymer φ^* at which the LC phase is formed is related to the asymmetry of a macromolecule x via the equation $\varphi^* = (1-2/x)8/x$, where x is the degree of asymmetry of the macromolecule (the length-to-diameter ratio of the molecule). The greater the molecular mass of the macromolecule, the higher the x and the lower the φ^* .

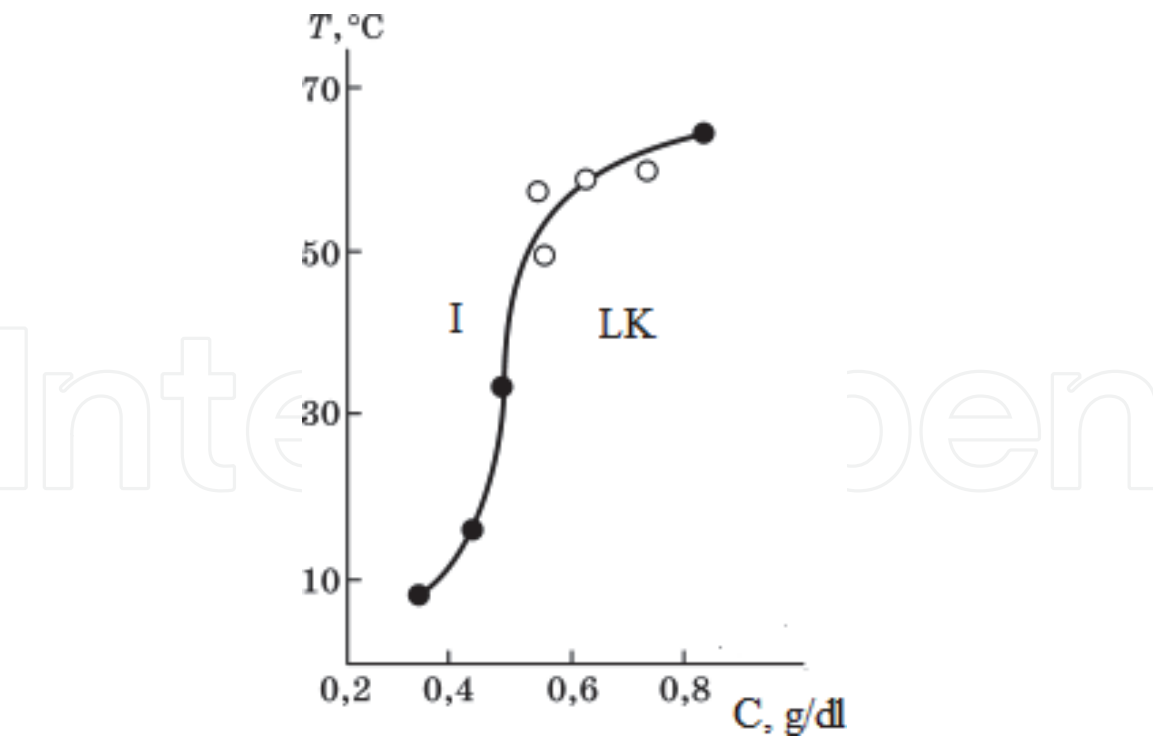


Figure 9.
Segment of the phase diagram of the cellulose tricarboxylate-methyl ethyl ketone system [49].

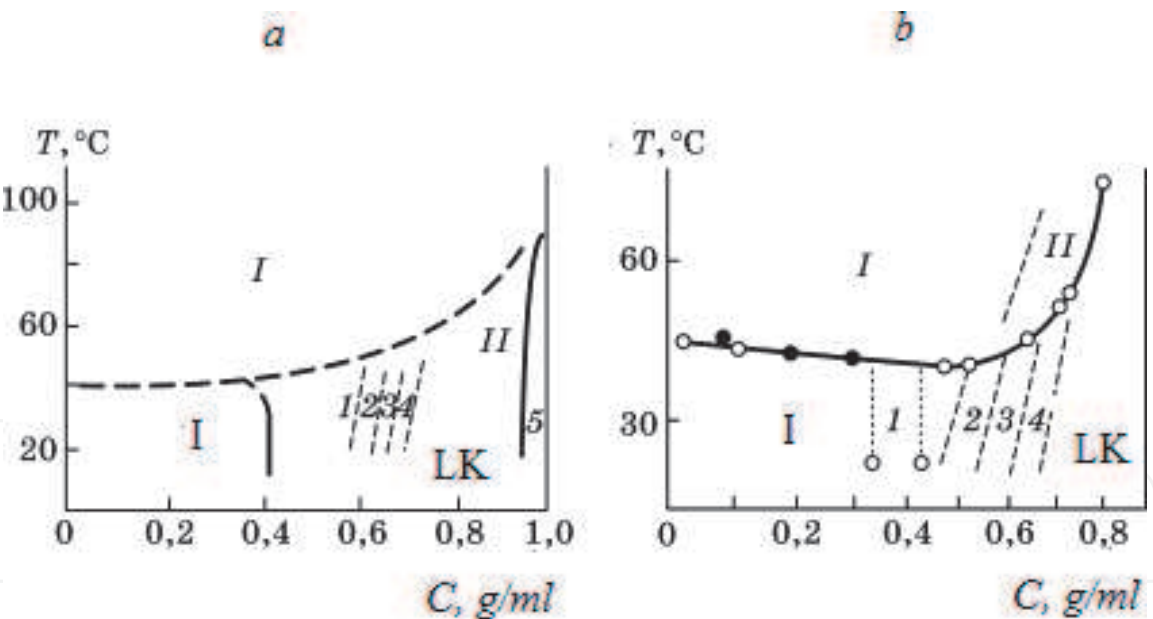


Figure 10.
Phase diagram of the hydroxypropyl cellulose (HPC)-water system [50] (a) and [51] (b): (1) turbid solution in case (a) and two-phase system in case (b); (2) red; (3) green; (4) violet; (5) transparent film. (I) Precipitation; (II) gel.

Figure 11 shows the boundary curves for the HPC-1-DMAA, HPC-3-DMAA, HPC-1-ethanol, HPC-2-ethanol, HPC-3-ethanol, HEC-1-water, and HEC-3-water systems. These curves separate transparent isotropic solutions (I) from opalescent anisotropic solutions (II) (ω_2 is the mass fraction of the polymer). It is shown that a rise in polymer molecular mass leads to a shift of the boundary curve to the region of lower concentrations. It should be noted that the Flory' theory does not consider influence of the chemical structure of polymer and solvent molecules on phase LC transitions.

Cellulose ether	Molecular mass	Degree of substitution, α
HPC-1	$M_w = 0.9 \times 10^5$	3.0
HPC-2	$M_w = 1.5 \times 10^5$	3.3
HPC-3	$M_\eta = 4.5 \times 10^5$	3.0
HPC-4	$M_w = 1.15 \times 10^6$	3.0
CEC	$M_w = 0.90 \times 10^5$	2.6
HEC-1	$M_w = 6.2 \times 10^4$	2.5
HEC-2	$M_w = 8.6 \times 10^4$	2.5
HEC-3	$M_\eta = 1.0 \times 10^5$	2.5
HEC-4	$M_\eta = 4.5 \times 10^5$	2.5
EC-1	$M_\eta = 2.6 \times 10^4$	2.6
EC-2	$M_w = 1.6 \times 10^5$	1.5
CENC	$[\eta] = 2.79 \text{ dL/g (DMAA, } T = 298 \text{ K)}$	0.19
MC	$M_\eta = 1.8 \times 10^5$	2.0
CEHEC	$M_\eta = 1 \times 10^5$	2.0

Table 2.
Characteristics of research objects.

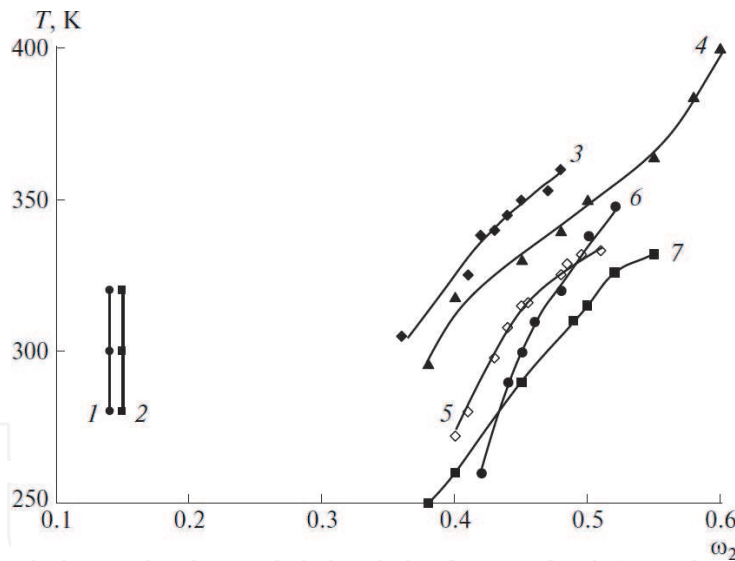


Figure 11.
Boundary curves of (1) HEC-4 ($M_\eta = 4.5 \times 10^5$)-water, (2) HEC-1 ($M_w = 6.2 \times 10^4$)-water, (3) HPC-4 ($M_w = 1.15 \times 10^6$)-ethanol, (4) HPC-2 ($M_w = 1.5 \times 10^5$)-ethanol, (5) HPC-4 ($M_w = 1.15 \times 10^6$)-DMAA, (6) HPC-1 ($M_w = 0.9 \times 10^5$)-ethanol, and (7) HPC-1 ($M_w = 0.9 \times 10^5$)-DMAA systems [52].

2.2 Effect of component nature on liquid-crystalline transitions in solutions of cellulose ethers

2.2.1 Effect of the chemical structure of polymer molecules on phase LC transitions

Figure 12 illustrates the data on phase transitions for the HPC-1-DMF and EC-1-DMF systems [52]. It is seen that the boundary curve of the EC-1-DMF system is in the region of lower concentrations than the boundary curve of the HPC-1-DMF system. Replacing the branched hydroxylpropyl radical with the ethyl radical

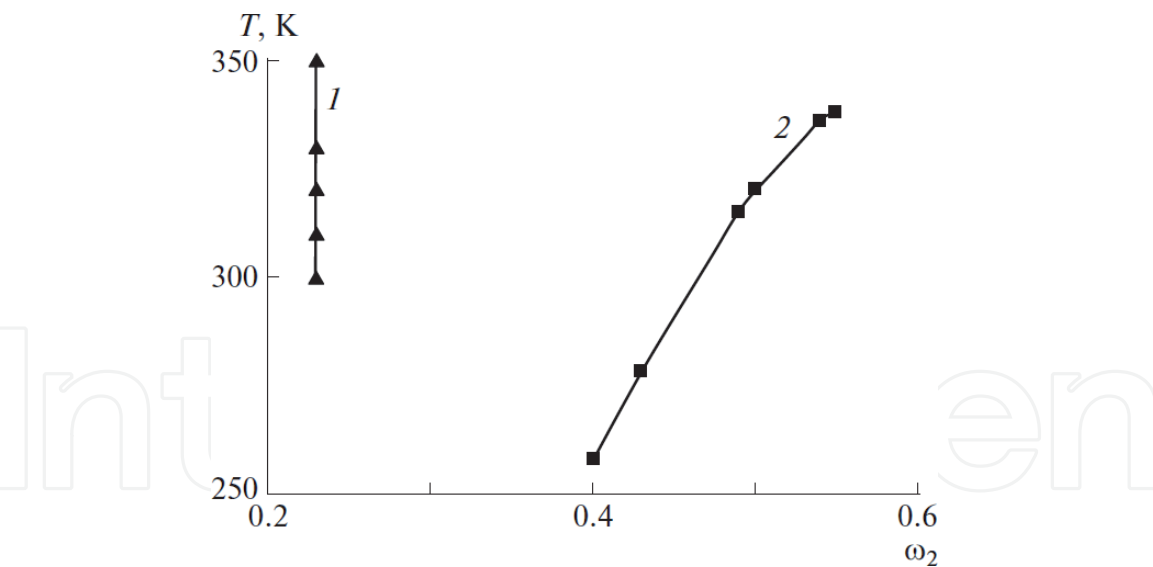


Figure 12.
Boundary curves of (1) EC-1 ($M_\eta = 2.6 \times 10^4$)-DMF and (2) HPC-1 ($M_w = 0.9 \times 10^5$)-DMF systems.

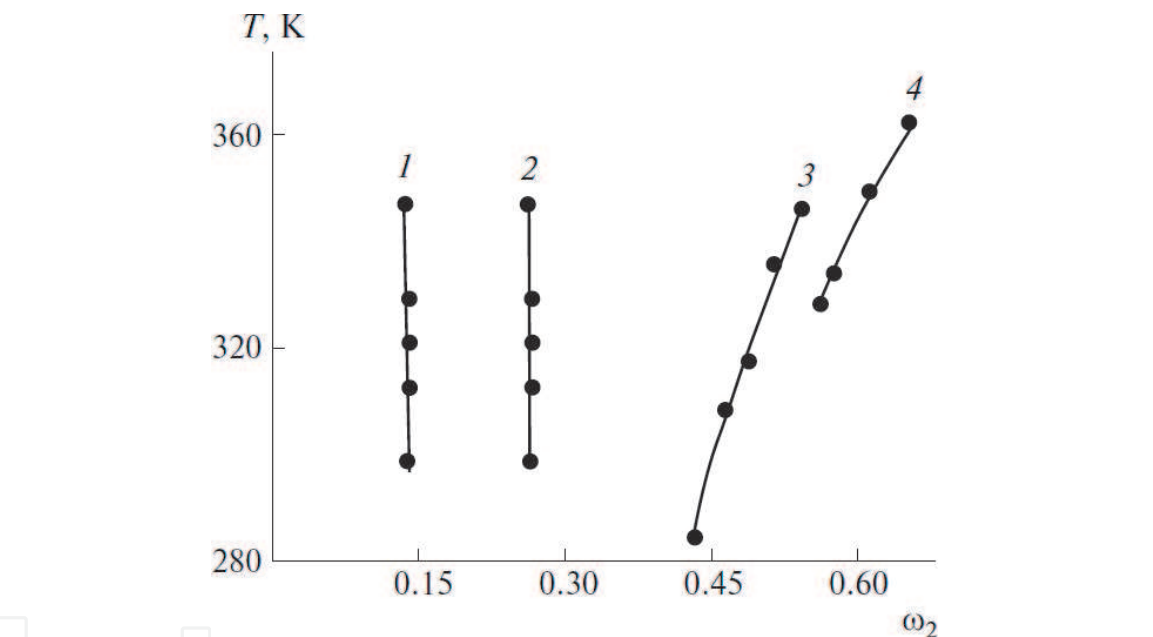


Figure 13.
Boundary curves of (1) EC-1 ($M_\eta = 2.6 \times 10^4$)-ethanol, (2) EC-1 ($M_\eta = 2.6 \times 10^4$)-DMF, (3) HPC-2 ($M_w = 1.5 \times 10^5$)-ethanol, and (4) HPC-2 ($M_w = 1.5 \times 10^5$)-DMSO systems.

enhances interaction between the units of neighboring macromolecules of the EC polymer, thereby facilitating formation of the LC phase. A lower polarity of EC-1 molecules worsens interaction with the polar DMF solvent.

Figure 13 shows the boundary curves of the EC-1-ethanol, EC-1-DMF, HPC-ethanol, and HPC-2-DMSO systems. It is shown, that, as for DMF solutions in **Figure 12**, in the case of ethanol solutions, the replacement of the hydroxypropyl radical with the ethyl radical in cellulose ether units causes a decrease in the concentration of formation of the LC phase.

A similar dependence is shown for the EC-1-DMF and HPC-2-DMSO systems. The boundary curves for the HPC-ethanol, HPC-DMAA, and HPC-DMSO systems change with temperature (**Figures 11–13**). At high temperatures the thermal motion of the molecules can disturb the liquid-crystalline order. Consequently, a high concentration of the polymer is required to retain the liquid-crystalline order. The boundary curves of the HEC-water (**Figure 11**), EC-DMF, and EC-ethanol

System ($\omega_2 = 0.05$)	d_w , nm	$(h^2)^{1/2}$, nm
CEC-DMAA	110	60
CEC-DMF	300	60
HPC-1-ethanol	320	64
HPC-1-water	180	64
HEC-1-water	1780	45
HEC-1-DMF	2480	45
HEC-2-DMF	1600	51
HEC-2-DMAA	1800	51
EC-2-DMAA	580	80

Table 3. Diameters d_w of light-scattering particles and mean-square distances between chain ends $(h^2)^{1/2}$ of cellulose ether macromolecules, $T = 298\text{ K}$.

systems (**Figure 13**) do not depend on temperature and are located in the region of lower concentrations. It is caused by a strong interchain interaction and a higher packing density of these macromolecules. The linear ethyl and hydroxyethyl radicals in the units of neighboring macromolecules can produce a denser packing with each other than the branched propyl radicals of HPC [53, 54]. The IR study of cellulose ether films showed [55] the formation of intra- and intermolecular hydrogen bonds with different strengths. It was shown that HEC is a more associated polymer than CEC and CEHEC. CEC is a less associated compound. CEHEC occupies the intermediate position. Methyl cellulose is also associated but to a lesser extent. As a result, large supramolecular particles are formed in EC and HEC solutions, which do not decompose under heating (**Table 3**).

The value of $d_w = 2r_w$, where r_w is the weight-average radius of particles scattering light, as determined by the turbidity spectrum method (this is described below). A comparison of the values of d_w and the sizes of macromolecules $(h^2)^{1/2}$ (**Table 3**) shows that, at a mass fraction of the polymer of $\omega_2 = 0.05$, light-scattering particles are supramolecular. The light-scattering particles of HPC and CEC consist of several macromolecules. The molecular-disperse solutions are not formed in the systems based on HEC and EC. Coarse light-scattering particles are probably the residues of the initial structure of the polymer stabilized by a great amount of strong hydrogen bonds formed between neighboring hydroxyl groups and a denser packing of linear ethyl and hydroxyethyl radicals in the units of neighboring macromolecules. Therefore, the position of the boundary curves for the EC-DMF and EC-ethanol systems does not depend on temperature.

Figure 14 shows the boundary curves of the CENC-DMAA, CENC-DMF, CEC-DMF, and CEC-DMAA systems. It is shown that, in the CENC solutions, the LC order appears at a lower concentration of the polymer. The introduction of a nitro group into CEC chain units increases the rigidity of chains; so the degree of asymmetry of macromolecules grows and the LC phase is formed at lower concentrations of the polymer.

The boundary curves for the aqueous solutions of HPC-1 and HEC-1 are given in **Figure 15**.

Obviously that the replacement of the hydroxypropyl radical with the hydroxyethyl one causes a substantial change in the phase diagram: first, the LC phase in HEC solutions is formed at lower concentrations. This is caused by the linear character and a smaller size of the hydroxyethyl radical compared with the hydroxypropyl one. So, interchain interaction is enhanced. Secondly, the LCST is absent in the HEC solutions. HPC contains 10–15% of the crystalline phase and

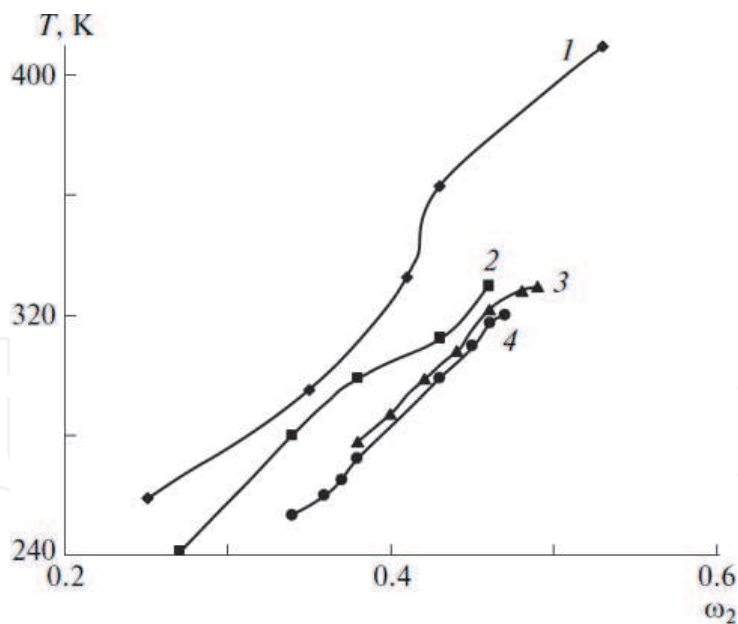


Figure 14.
Boundary curves of (1) CENC-DMAA, (2) CENC-DMF, (3) CEC ($M_w = 0.9 \times 10^5$)-DMF, and (4) CEC ($M_w = 0.9 \times 10^5$)-DMAA systems [52].

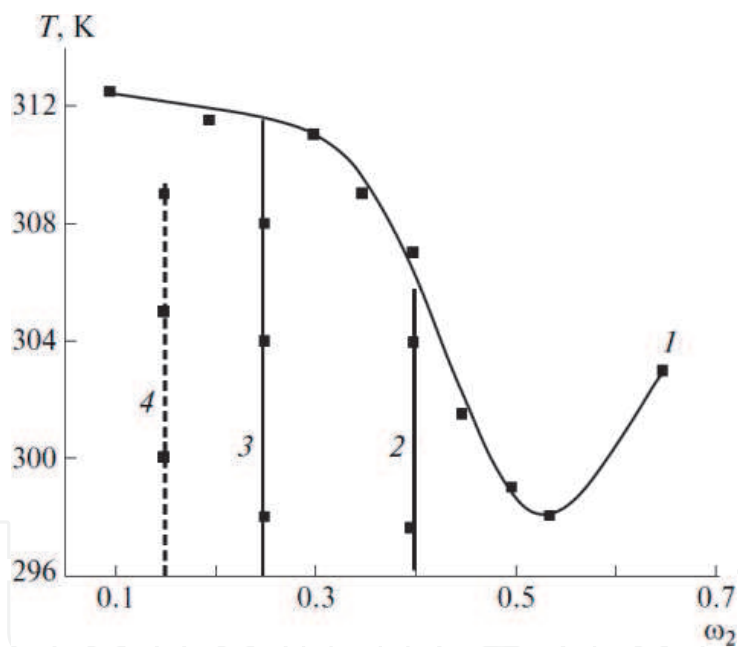


Figure 15.
Boundary curves of (1–3) HPC-1 ($M_w = 0.9 \times 10^5$)-water and (4) HEC-1 ($M_w = 6.2 \times 10^4$)-water systems. Lines 3 and 4 are the boundaries of the isotropic-anisotropic solution transition, and lines 2 and 3 restrict the region of coexistence of isotropic and anisotropic phases [52].

90–85% of the vitrified cholesteric LC phase [56, 57]. The degree of crystallinity of HEC is almost zero. Structural changes during dissolution of HPC in water may be caused by the melting of crystalline domains and relaxation of the metastable glass-like structure. For HEC, only relaxation of the metastable glass-like structure can be observed. The interactions of HPC with water are determined both by the salvation of macromolecules by water owing to the formation of hydrogen bonds [58] and the “hydrophobic hydration” of water itself [59]. The latter process includes the compaction of water structure during penetration of nonpolar molecules or their fragments into voids in its structure. Methyl and methylene groups of HPC are nonpolar fragments. Therefore, intermolecular distances in water decrease, the interaction

between its molecules becomes stronger, the exothermic effect of dissolution grows, and the entropy of mixing decreases [60]. The interactions of both types contribute to the negative enthalpy and entropy of mixing of HPC with water. Phase separation of the HPC-water system during heating may be caused by the melting of the densified water structure around hydrophobic fragments of the polymer [61]. The interactions of HEC with water can also be determined both by the solvation of macromolecules by water and by the “hydrophobic hydration” of water itself. However, since there are no methyl groups in HEC molecules to a lesser extent the LCST is absent for this system.

Figure 16 shows the boundary curves of the HEC-2-DMAA, EC-DMAA, and HPC-1-DMAA systems.

The solutions of HEC, EC, and HPC in DMAA follow the same shift in the boundary curves as water and ethanol solutions because of the reasons described above. The replacement of the hydroxyethyl radical in HEC with the ethyl radical in EC causes the weakening of interaction owing to a decrease in the possible formation of hydrogen bonds and, as a result, owing to a rise in concentration of LC phase formation. Note that the boundary curves for the solutions of HEC and EC are in the region of lower concentrations than the solutions of HPC. This is connected with the presence of bulky branched hydroxypropyl radicals in molecules. The boundary curves for the HEC-1-DMF, CENC-DMF, CE-DMF, and HPC-1-DMF systems are presented in **Figure 17**. For the solutions of these polymers in DMF, the same regularities as for the solutions in DMAA are observed.

2.2.2 Effect of the chemical structure of solvent molecules on phase liquid crystalline transitions

Figures 18–20 show the boundary curves for HPC and CEC solutions. The position of the boundary curves on the composition significantly depends on the solvent nature. The better the solvent, to a lesser degree it deteriorates the initial structure of the polymer. Therefore, the LC phase in solution will form at a higher polymer concentration. A more polar solvent should be better for polar cellulose ethers.

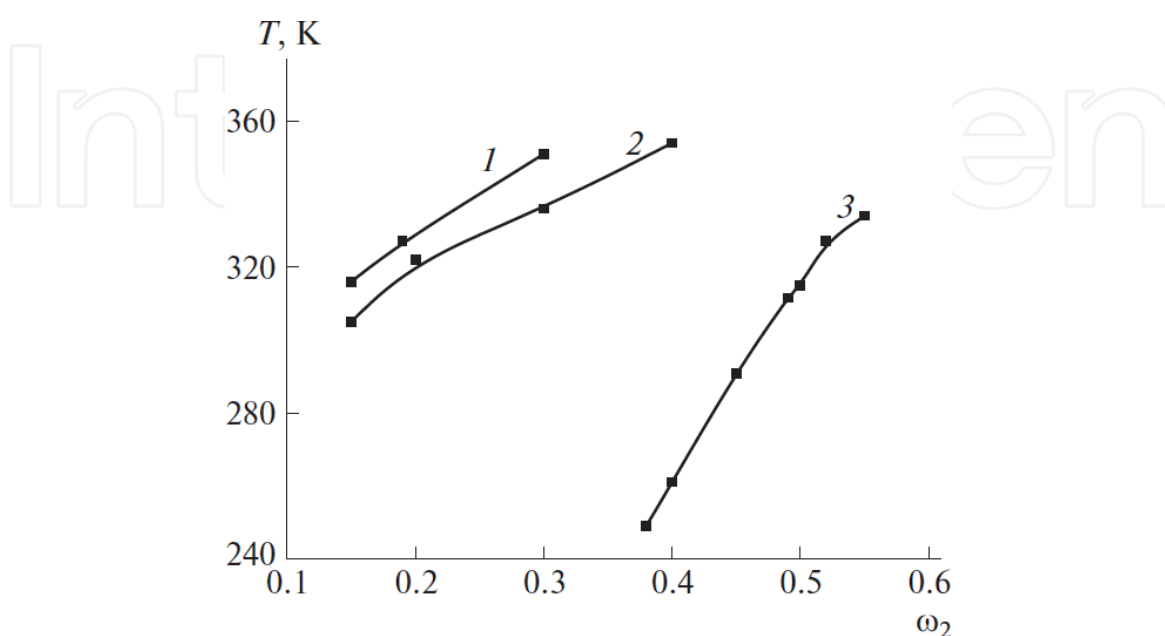


Figure 16.

Boundary curves of (1) HEC-2 ($M_w = 8.6 \times 10^4$)-DMAA, (2) EC-2 ($M_w = 1.6 \times 10^5$)-DMAA, and (3) HPC-1 ($M_w = 0.9 \times 10^5$)-DMAA systems [52].

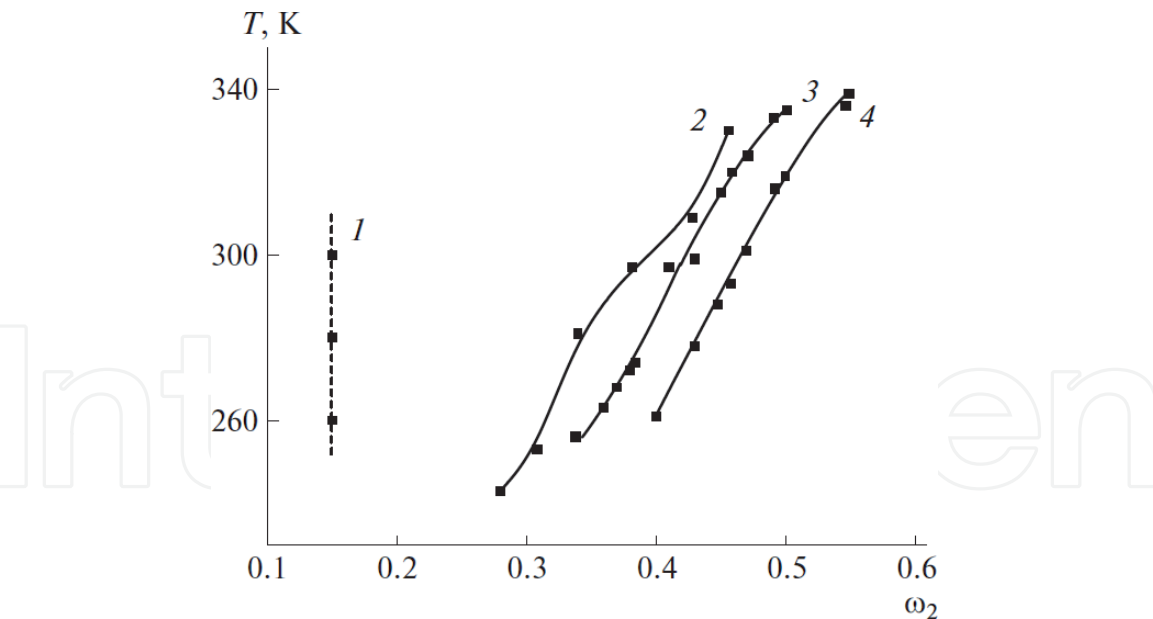


Figure 17.
 Boundary curves of (1) HEC-1 ($M_w = 6.2 \times 10^4$)-DMF, (2) CENC-DMF, (3) CEC ($M_w = 0.9 \times 10^5$)-DMF, and (4) HPC-1 ($M_w = 0.9 \times 10^5$)-DMF systems [52].

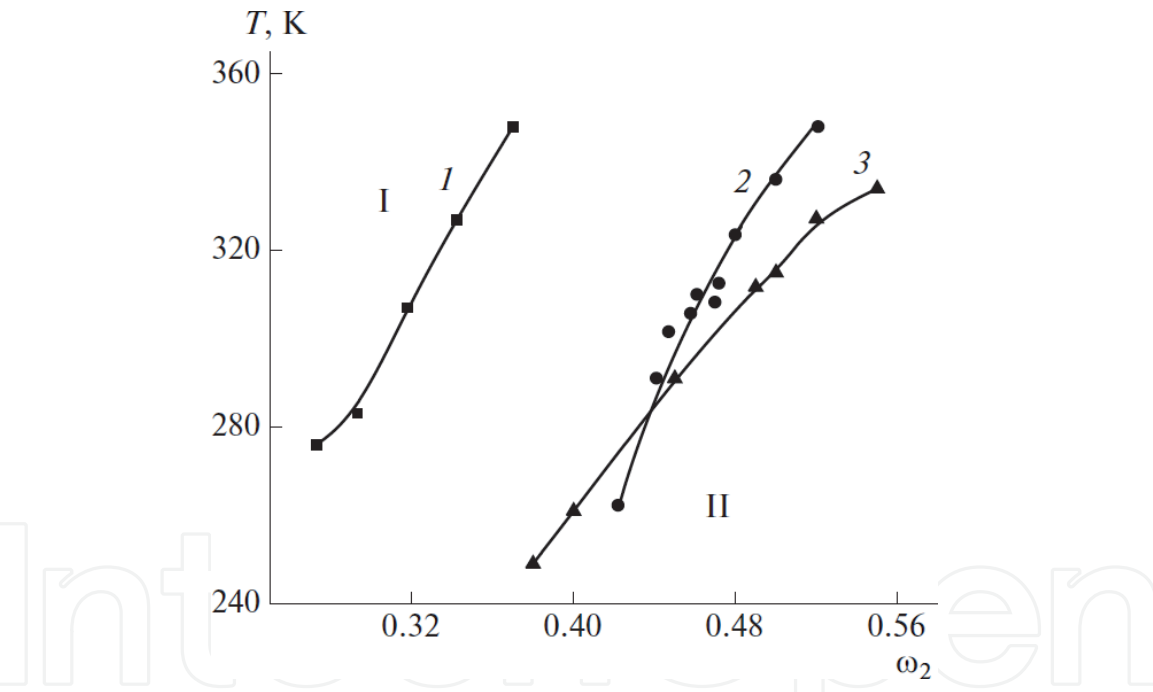


Figure 18.
 Boundary curves of (1) HPC-1 ($M_w = 0.9 \times 10^5$)-acetic acid, (2) HPC-1 ($M_w = 0.9 \times 10^5$)-ethanol, and (3) HPC-1 ($M_w = 0.9 \times 10^5$)-DMAA systems [52].

Table 4 compares the second virial coefficients and dipole moments of solvent molecules. An increase in the polarity of solvent molecules entails a rise in second virial coefficients, suggesting the improvement of thermodynamic interaction of the components.

Here and in **Figures 19** and **20**, I refers to the region of isotropic solutions, and II refers to the region of anisotropic solutions.

Figure 13 shows that the boundary curve of the HPC-2-ethanol system is in the region of lower concentrations than the curve of the HPC-2-DMSO system. This may be caused by different polarities of solvent molecules. The dipole moment of ethanol molecules $\mu = 1.69$ D [63] is lower than the dipole moment of DMSO

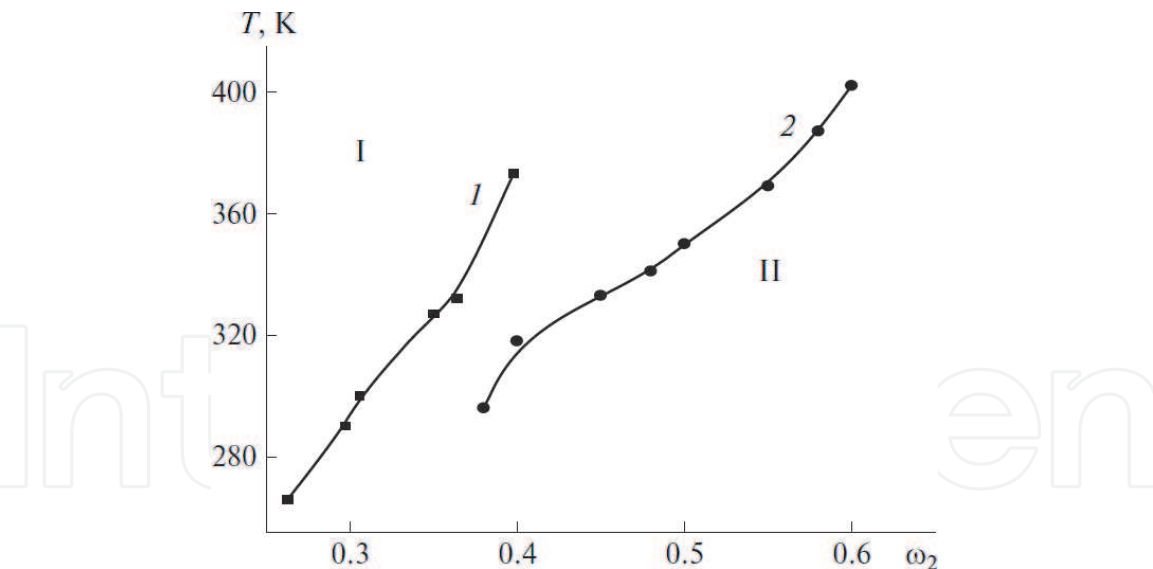


Figure 19. Boundary curves of (1) HPC-2 ($M_w = 1.5 \times 10^5$)-acetic acid and (2) HPC-2 ($M_w = 1.5 \times 10^5$)-ethanol systems [52].

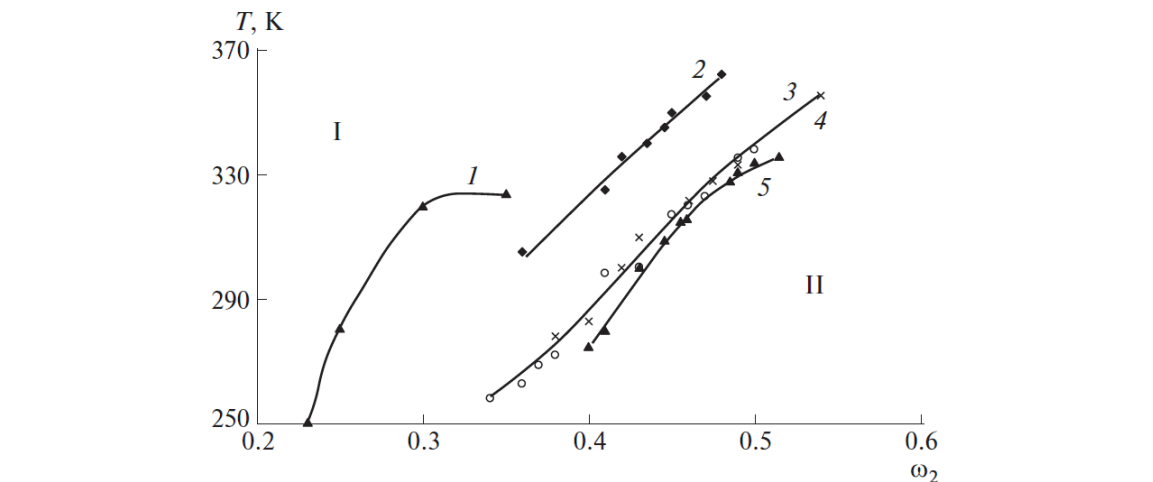


Figure 20. Boundary curves of (1) CEC ($M_w = 0.9 \times 10^5$)-TFAA/MEC, (2) HPC-4 ($M_w = 1.15 \times 10^6$)-ethanol, (3, light circles) CEC ($M_w = 0.9 \times 10^5$)-DMF, (4) CEC ($M_w = 0.9 \times 10^5$)-DMAA, and (5) HPC-4 ($M_w = 1.15 \times 10^6$)-DMAA systems (TFAA/MEC is trifluoroacetic acid/methylene chloride, 1/1 volume fractions) [52].

Solvent	$A_2 \times 10^4 \text{ cm}^3 \text{ mol/g}^2$	Dipole moment, D
DMAA	7.5	3.86
Water	3.1	1.68
Formamide	8.4	3.7

Table 4. Second virial coefficients and dipole moments of solvent molecules for cellulose acetate solutions [62].

$\mu = 3.96 \text{ D}$ [63]. A more polar solvent DMSO destroys the initial structure of the polar polymer to a greater extent; therefore the sizes of supramolecular particles decrease and a higher concentration of polymer is needed for formation of the LC order in solutions. A similar behavior is observed for the EC solutions. The dipole moment of DMF molecules $\mu = 3.81 \text{ D}$ [63] is higher than the dipole moment of ethanol molecules

Polymer	Solvent	μ , D [63]	$-\Delta g^m$, J/mol solution [60]
MC	Chloroform	1.06	1400
	H ₂ O	1.83	1350
	Ethanol	1.69	1200
CEC	Chloroform	1.06	1400
	H ₂ O	1.83	1250
	Acetone	2.85	1400
	Ethanol	1.68	900
CEHEC	Chloroform	1.06	1400
	TFAA	2.28	4250
	H ₂ O	1.83	1150
	Dioxane	0.45	1250
	Acetone	2.85	1700
HEC	Chloroform	1.06	1300
	H ₂ O	1.83	1700
	Ethanol	1.68	1050
	Dioxane	0.45	300

Table 5.
Dipole moments and minimum Gibbs energies of mixing of cellulose ethers with low-molecular-mass liquids.

$\mu = 1.69$ D, and the LC state forms in the EC -DMF system at a higher polymer concentration. **Table 5** compares the thermodynamic parameters of interaction for the cellulose ether-solvent systems and the physical properties of the solvents [60, 63].

The dissolving capacity of water is due to the possibility to form hydrogen bonds between its molecules and molecules of polymers. For HEC containing the maximal amount of hydroxyl groups, water is the best solvent.

The good interaction with chloroform and water is characteristic of MC, the least associated polymer with a small nonpolar substituent and unsubstituted hydroxyl groups. CEC and CEHEC containing polar nitrile groups with donor properties [64] have a high affinity for chloroform and a low affinity for water despite the presence of unsubstituted hydroxyl groups. Owing to a high packing density and, as a result, strong interchain interaction, CEC does not dissolve but only limitedly swells in water. This may suggest an insignificant role of hydrogen bonds in dissolving cyanoethylated ethers. This assumption is confirmed by a low affinity of CEC for ethanol. Dioxane being the electron donor for polymer molecules [64] capable of H bonding has a low thermodynamic affinity for HEC and CEHEC.

With some exceptions, the higher the dipole moment of solvent molecules, the more negative the Gibbs energy of mixing, i.e., the better the solubility of the cellulose ethers. Thus, in a first approximation, the dipole moment can be used as an estimate of solvent quality for cellulose ethers.

3. Self-assembly of nanodimensional molecules of cellulose ethers

An important specific task to be solved within the priority direction of science and technology—industry of nanosystems and materials—as well as in critical technology—nanotechnologies and nanomaterials—is the study of the process of self-assembly

of supramolecular systems. Such systems include the solutions of rigid chain polymers, the molecules of which exhibit an ability for self-organization leading to the formation of liquid crystalline phases. Informative methods employed for the research of solution structures are the optical methods: the method of Rayleigh light scattering, the method of dynamic light scattering, the method of measurement of optical density (turbidimetry). The chapter presents the results of the examination of solution structure using the turbidity spectrum method, which makes it possible to determine the size of supramolecular particles in solutions in a wide composition range. The method was introduced by Heller et al. [65–67] and further developed by Klenin et al. [68]. According to this method, the typical dependence of logarithm of optical density A on the logarithm of wavelength required for computation of r_w is described by straight line. The decrease of A with the increase of wavelength λ is observed, which is in agreement with Angstrom's Eq. $A \sim \lambda^{-n}$. Wavelength exponent n depends on the size of light scattering particles and is connected with parameter $\alpha = 2\pi r_w / \lambda_{\text{average}}$ and relative refractive index $m_{\text{rel}} = n_{\text{dpolymer}} / n_{\text{dsolvent}}$. Value $\lambda_{\text{average}} = \lambda_0 / n_{\text{dsolvent}}$ (λ_0 is the wavelength of light in vacuum corresponding to the middle of the linear section of the plot $\ln A = f(\ln \lambda)$, r_w is the weighted average of particle radius). The slope of the lines $\ln A = f(\ln \lambda)$ was used to identify n and then α for the given m_{rel} and r_w [68].

Figure 21 shows the concentration dependencies of optical density A (for $\lambda = 490$ nm) experimentally obtained at 298 K for the systems: HEC-2-DMF and HEC-1-DMF. The dashed line separates the region of isotropic (I) solution from the region of anisotropic (II) solution. The similar dependences were obtained for HPC-1-ethanol, HPC-1-water, HEC-1-water, HEC-3-water, CEC-DMAc, HEC-2-DMAc, and EC-DMAc systems. These diagrams show that as the concentration increases, the optical density increases also. This indicates the process of structure formation in the systems, which must manifest itself through the increase in the size of light scattering particles r_w . As is evident from the comparison with phase diagrams, the increase of A is the most abrupt at the LC phase formation.

The concentration dependencies of the calculated average weighted radii of supramolecular particles at 298 K are given in **Figure 22**. The similar dependences were obtained for the HEC-1-water, HEC-3-water (2), HPC-water HEC-1-DMF, HEC-2-DMF, HEC-2-DMA, and EC-DMAc systems.

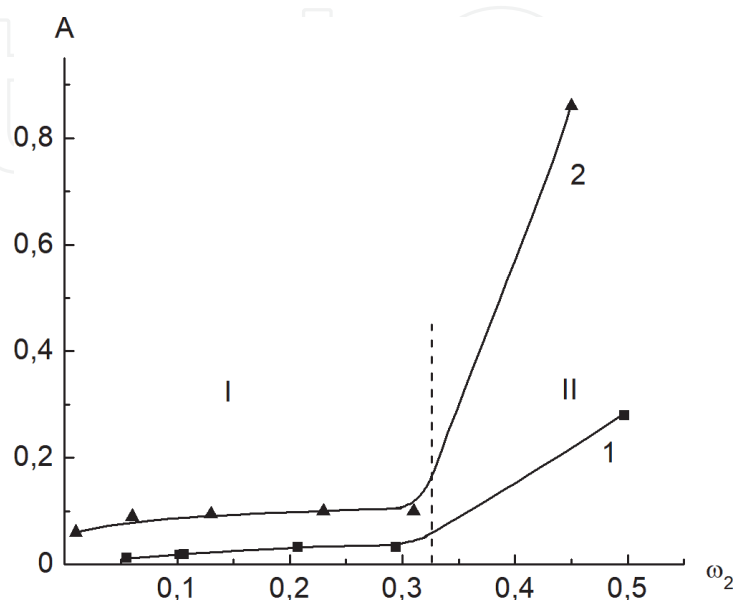


Figure 21. Concentration dependencies of the optical density for HEC-2-DMF (1) and HEC-1-DMF (2) systems: (I) isotropic solutions, (II) anisotropic solutions.

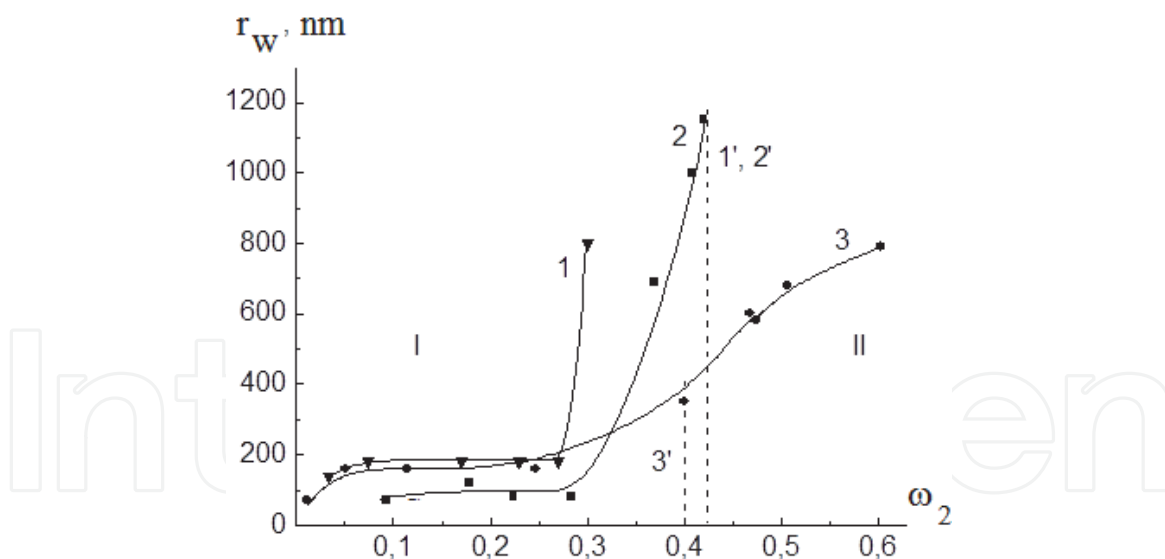


Figure 22.
Concentration dependencies of the sizes of light scattering particles for the systems: CEC-DMF (1), CEC-DMAc (2), HPC-1-ethanol (3). (1', 2', 3') the phase boundaries [12].

According to **Table 3** and **Figure 22** for the systems: CEC-DMAc, CEC-DMF, HPC-ethanol, HPC-1-water, HEC-3-water at polymer concentration of up to $\omega_2 \approx 0.05$, the diameters of light scattering particles do not exceed 320 nm, for the EC-DMAA system, they are of 580 nm and for the HEC-1-water, HEC-1-DMF, HEC-2-DMF, and HEC-2-DMAc systems, they vary from 1600 to 2500 nm. The calculated values $(h^2)^{1/2}$ show that the light scattering particles contain several macromolecules, except for the systems based on HEC where the molecular-dispersed solutions are unlikely to occur. According to studies [48], if the hydroxyl groups in cellulose macromolecules are completely substituted, their solubility at a molecular level is observed, while the partial substituted cellulose derivatives, as a rule, do not dissolve up to single macromolecules. The big light scattering particles are probably the residues of initial polymer structure stabilized by many strong hydrogen bonds between neighboring hydroxyl groups. After partial substitution, a certain portion of such bonds remains undisturbed by a solvent and large aggregations are found in the solutions. In [69] the size of light scattering particles was determined using the light scattering method. It was shown that in the solutions of samples of methyl hydroxypropyl cellulose and methyl hydroxyethyl cellulose, with M varying from 10^3 to 10^6 in water and cellulose acetate in acetone, the average number of aggregated molecules in the particles in diluted solutions grows from 10 to 10^3 . In diluted water solutions of methylcellulose with a polymerization degree of 120, there are aggregations comprising 4000 macromolecules [70].

The sharpest increase of particle sizes is observed in the LC phase. It should be noted that for all studied systems, the $r_w = f(\omega_2)$ curves exhibit a horizontal section in a certain concentration range indicating the constant size of supramolecular particles. The obtained data made it possible to suggest the following mechanism of self-assembly of cellulose ester macromolecules preceding LC transition. In diluted solutions there exist associates, including several macromolecules. Within the concentration range up to $\omega_2 \approx 0.05$, supramolecular particles of a stable-sized “packet” are formed. The term “packet” has been used in physics for a long time. For example, the wave packet is a certain summation of waves limited spatially and by time. Thus, in quantum mechanics, the description of a particle as a wave packet contributed to the acceptance of statistic interpretation of the square of absolute value of wave function.

Here the term “packet” means a stable supramolecular particle with essentially stable dimensions, which is a nuclei of the new LC phase. These supramolecular particles contain both polymers and conjugated solvents. As is shown in **Figure 22**, in the region of moderately concentrated solutions, the “packet” dimensions remain virtually unchanged within a certain concentration range, depending on the system. As the concentration of polymer in solutions further increases, the number of packets also increases while their size does not change. The transition of the system to a fully LC state is induced by the aggregation of packets with the formation of large particles thousands of nanometers in size. It is obvious that these large particles include a great number of macromolecules.

3.1 Effect of magnetic field on size of supramolecular particles in solutions of cellulose derivatives

To study the influence of magnetic field on the size of supramolecular particles, a cell with the polymer solution was placed in a gap between the electromagnet

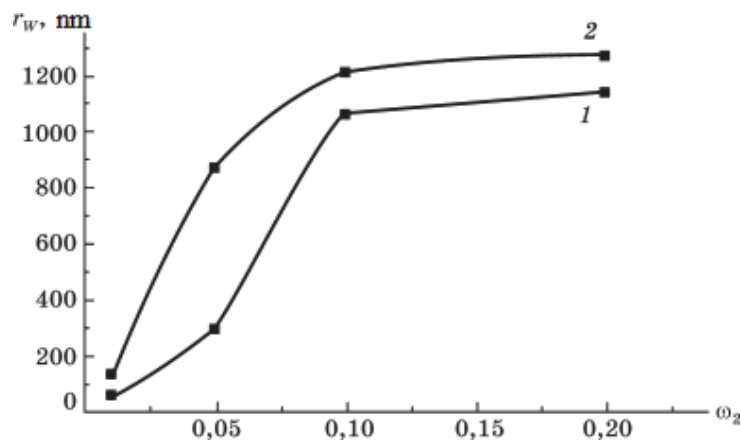


Figure 23. Concentration dependence of radii of light-scattering particles in the EC-DMAc system: (1) before and (2) after magnetic-field treatment. $H = 9 \text{ kOe}$ [12].

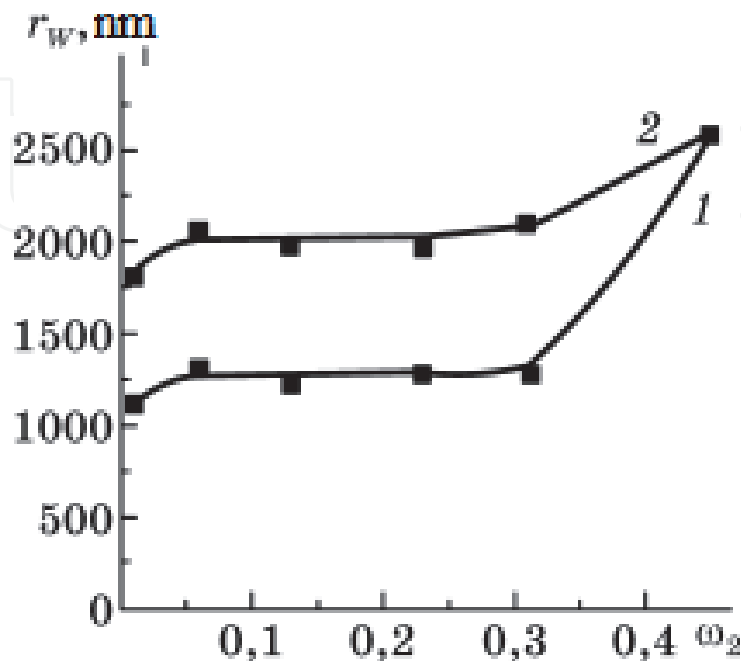


Figure 24. Concentration dependencies of radii of light-scattering particles in the HEC-1-DMF system: (1) before and (2) after magnetic-field treatment. $H = 9 \text{ kOe}$ [12].

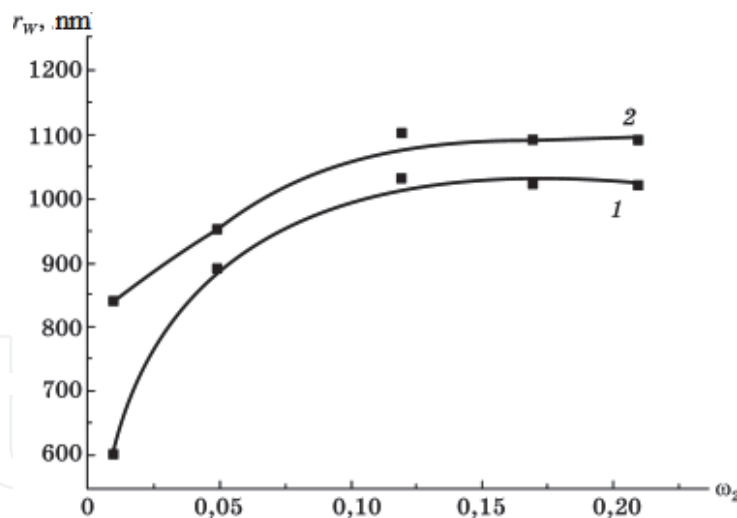


Figure 25. Concentration dependencies of radii of light-scattering particles in the HEC-1-water system: (1) before and (2) after magnetic-field treatment. $H = 9 \text{ kOe}$ [12].

poles and kept at a field intensity of 9 kOe for 50 min. The optical density was measured within 5–10 min after the magnetic field was turned off.

It was shown that the EC-DMAc, HEC-1-DMF, and HEC-1-water systems exhibit an increase in optical density after magnetic-field treatment. The increase in the optical density of solutions is indicative of the occurrence of an additional association of macromolecules because they are oriented by their axes concerning lines of magnetic field.

It was revealed that the magnetic field leads to the increase in the radii of light-scattering particles in solutions. The concentration dependences of the sizes of supramolecular particles for the EC-DMAc, HEC-1-DMF, and HEC-1-water systems are presented in **Figures 23–25**.

4. Phase transitions of liquid crystalline systems in magnetic field

Experiments in the magnetic field were performed using a setup generating a constant magnetic field with a strength up to 15 kOe [12]. A sealed ampoule with a polymer solution, which was transparent at elevated temperatures, was placed into a gap between magnet poles. The vector of the magnetic field strength was directed normal to the solution layer ($\sim 5\text{-mm}$ thick). The solution was cooled using a thermostating jacket, and the onset temperature of opalescence development was recorded. This temperature T_{ph} was related to the appearance of the LC state. The type of the phase transition was determined with the use of the polarization-photoelectric setup [12]. The sealed ampoule containing a transparent solution was placed into a gap between crossed polaroids (a polarizer and an analyzer). The ampoule was cooled using the thermostating jacket. A light beam from a helium-neon laser was transmitted through the polaroids in the direction normal to the ampoule containing the solution. When the solution was transparent (isotropic), the intensity of the transmitted light was zero. As the system became turbid upon cooling, the transmitted light intensity increased, as measured with a photoresistor. This fact suggested formation of an anisotropic phase, that is, the LC phase transition.

The phase diagrams were obtained under magnetic field for the systems: HPC-ethanol, HPC-DMAc, HPC-water, CEC-DMAc, CEC-DMF, PBG-DMF. The LC solutions of the cellulose esters exhibited the increase in the temperature of phase

LC transition in the magnetic field and the preservation of the increased temperature for many hours after the magnetic field was switched off. This means that the cellulose ether-solvent systems are the “systems with memory.” **Figures 26–28** show the results of the experiments [12].

It is observed that the magnetic field increases the temperature of LC phase transition. On the basis of the data from other studies, it seems to be induced by the change in the liquid crystalline type, in particular, by the LC cholesteric → LC nematic phase transition.

Figures 26–28 show that in the course of the time, the phase LC transition temperature increased by the magnetic field goes back down to the initial value (prior to the exposure to magnetic field). This means that the thermal motion destroys the field-induced orientation of macromolecules. The higher the temperature of thermostatic control of the solutions, the more intensive the thermal movement and the faster the recovery of the initial structure of solutions.

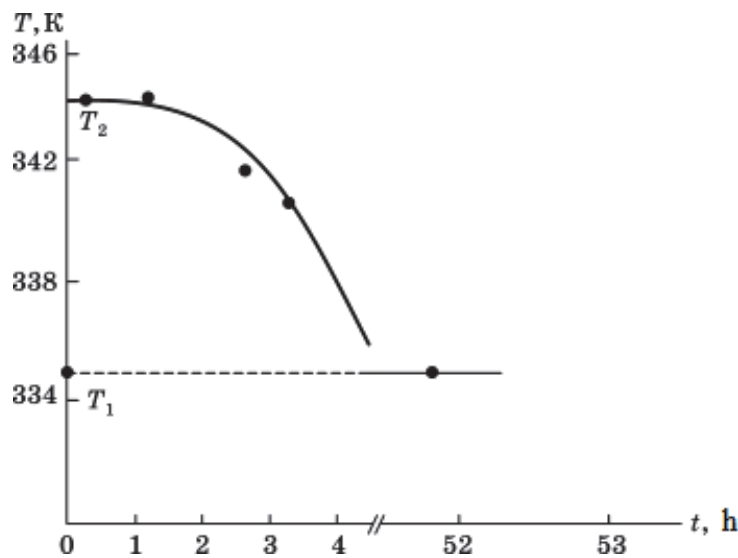


Figure 26. Time dependence of T_{ph} for HPC-2 solution in DMAc ($\omega_2 = 0.51$) at $T = 370$ K after the influence of magnetic field with intensity of 7 kOe. T_1 is the temperature of the LC transition without the field. T_2 is the temperature of the LC transition under the field.

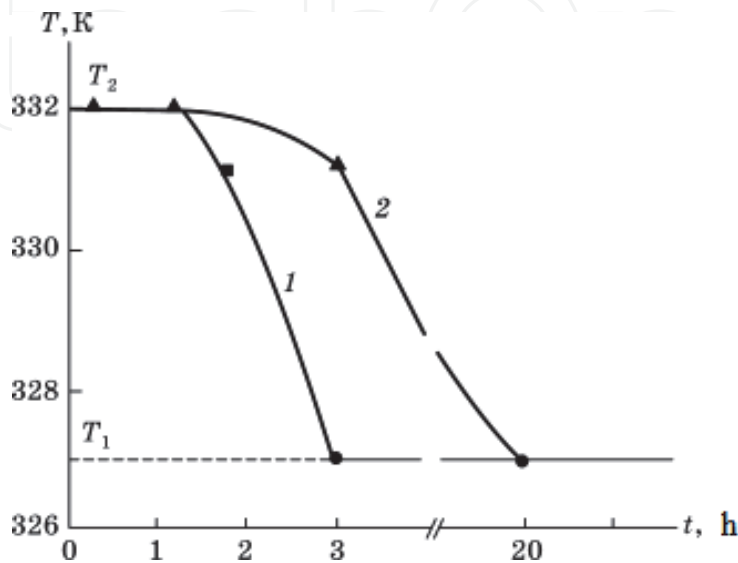


Figure 27. Time dependencies of T_{ph} for CEC solution in DMAc ($\omega_2 = 0.48$) at $T = 370$ (1) and 298 K (2) after the influence of magnetic field with intensity of 7 kOe. T_1 is T_{ph} at $H = 0$ kOe, T_2 is T_{ph} at $H = 7$ kOe.

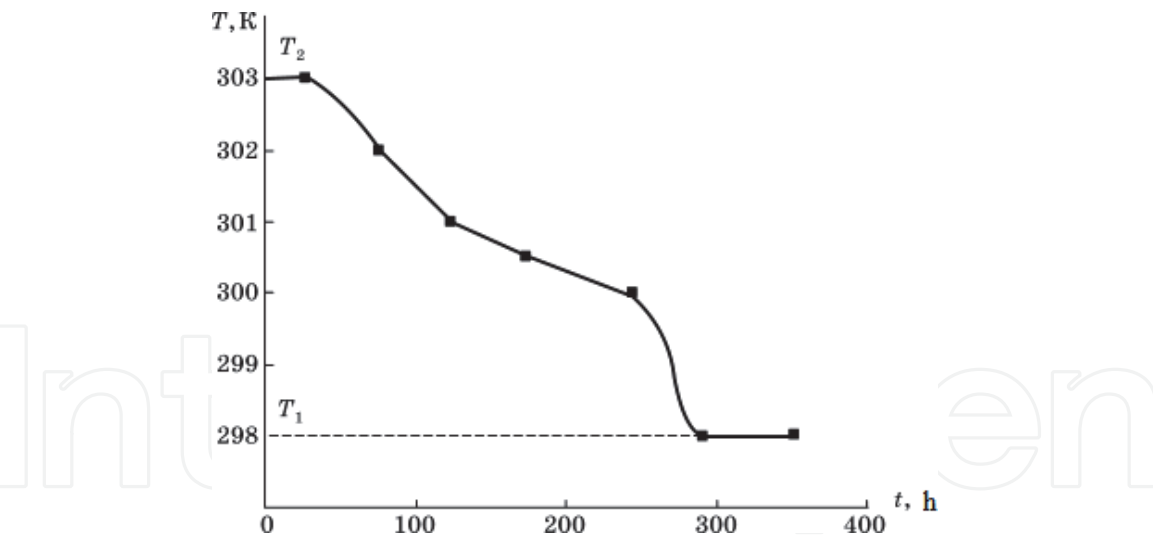


Figure 28.
Time dependence of T_{ph} for HPC-1 solution in water ($\omega_2 = 0.54$) at $T = 298\text{ K}$ after the influence of magnetic field with intensity of 5 kOe. T_1 is T_{ph} at $H = 0\text{ kOe}$, T_2 is T_{ph} at $H = 5\text{ kOe}$.

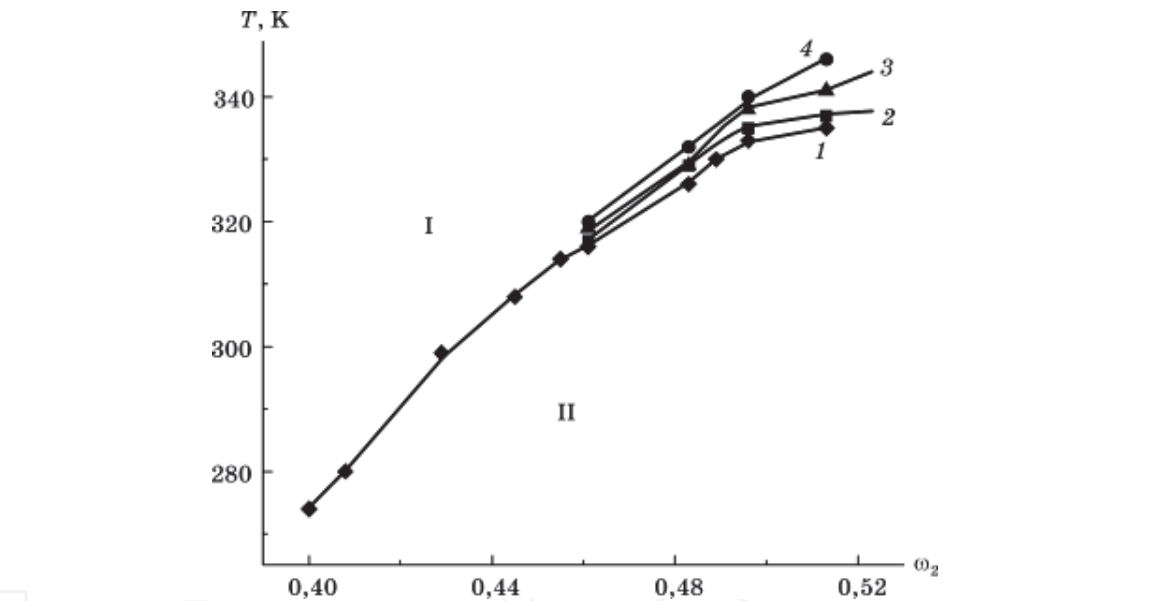


Figure 29.
Boundary curves of HPC-1-ethanol. $H = 0$ (1), 3 (2), 5 (3), and 9 (4) kOe.

The boundary curves of the cellulose ether-solvent systems in the magnetic field are presented in **Figures 29–32** [12] (I is the region of isotropic solutions, II is the region of anisotropic solutions).

Figures 29–32 show that the magnetic field leads to the boundary curve shift to the region of the higher temperatures. Thus, the anisotropic (II) region extends and isotropic region (I) gets narrow, and in the case of the HPC-1-water system, the region of amorphous phase separation becomes narrow. The observed effects are related to the change in macromolecule orientation under a magnetic field.

The shift of the boundary curves of the studied systems depends on the intensity of the magnetic field and polymer concentration, as discussed below.

Figure 33 shows the diagrams of ΔT dependence on the magnetic field intensity (H) for the HPC-3-DMAc system, where ΔT is the difference between the temperatures of the phase LC transition in the magnetic field and in its absence [12].

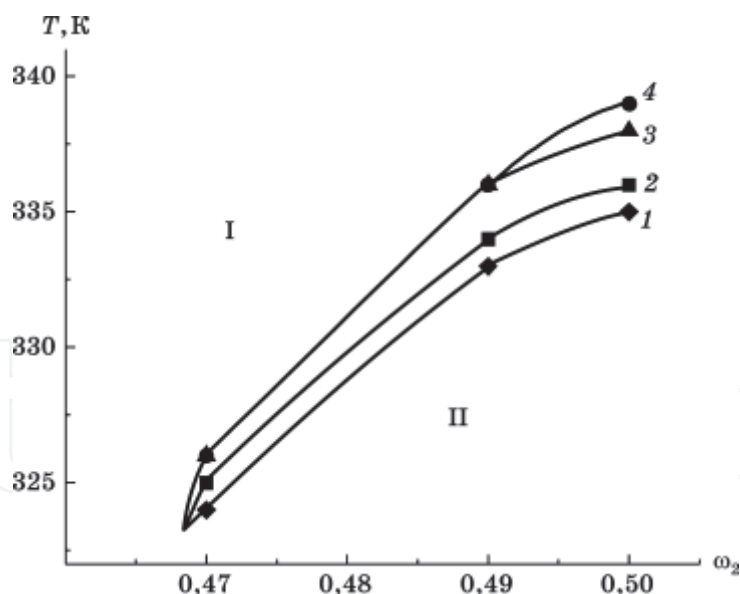


Figure 30.

Boundary curves of CEC-DMF system. $H = 0$ (1), 3 (2), 5 (3), and 9 kOe (4).

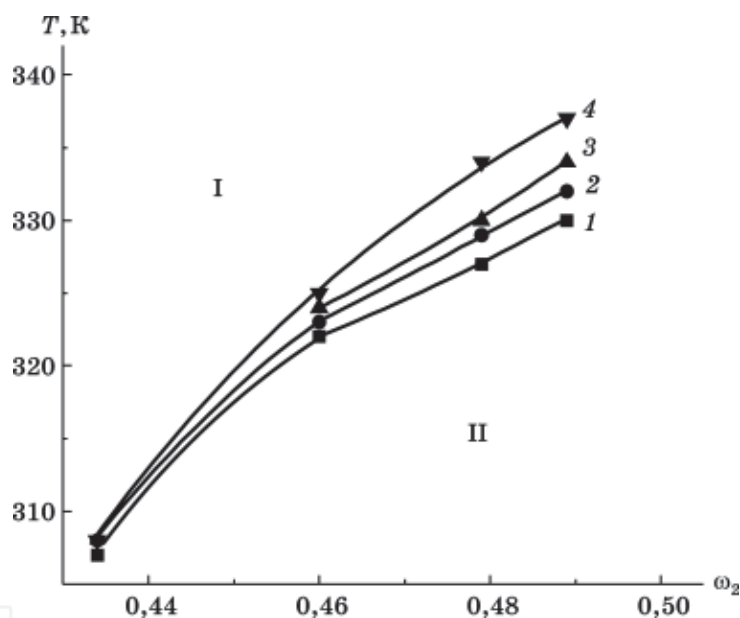


Figure 31.

Boundary curves of CEC-DMAc system. $H = 0$ (1), 3 (2), 5 (3), and 9 kOe (4).

The similar behavior is observed for all given systems (except for the HPC-1-water system): the greater the intensity of the magnetic field, the more the macromolecule orientation and the higher the temperature of the LC phase transition. For the HPC-1-water system, the inverse dependence is observed: the higher the value of H , the lower the ΔT . Probably this is associated with the specific character of the solvent and with the other type of the phase transition upon heating.

The effect of the polymer concentration on magnetic-field-induced changes in phase transition temperatures is due to two factors: (1) as concentration increases, the number of macromolecules capable of orientation in the magnetic field grows; as a consequence, the temperature of the phase LC transition should increase; (2) polymer concentration growth leads to the increase in viscosity and in the interchain interaction that hampers the development of the orientation processes and weakens the impact of the magnetic field. In general, the dependence of ΔT on concentration seems to be described by a curve with a maximum similar to the curve of the HPC-1-water system.

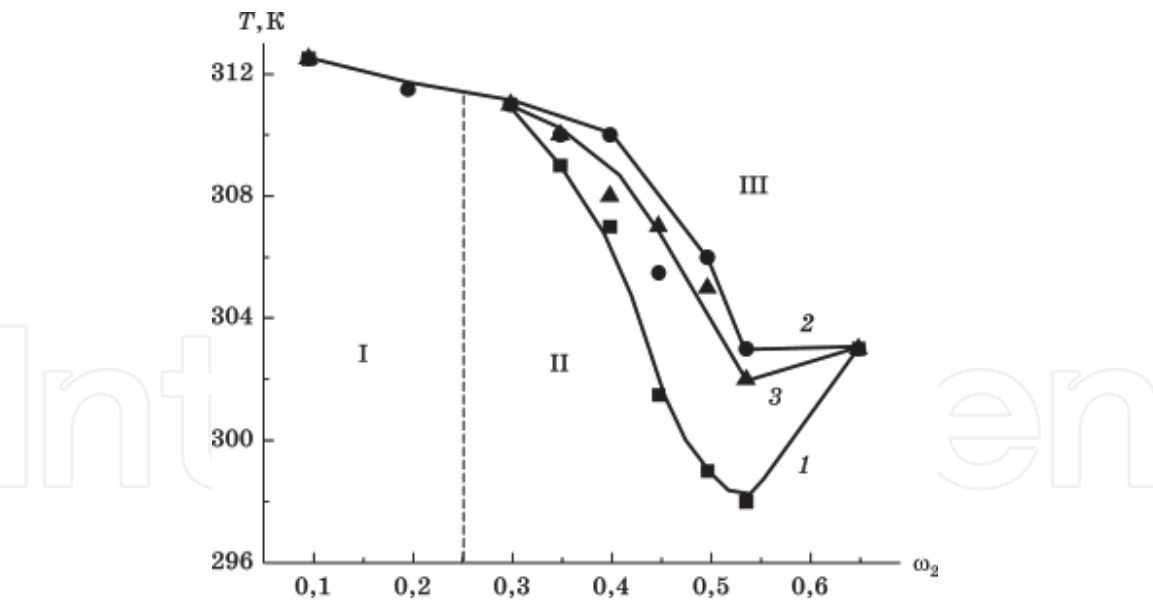


Figure 32.
Boundary curves of HPC-1-water. $H = 0$ (1), 5 (2), and 9 (3) kOe. I is the region of isotropic solutions, II is the region of anisotropic solutions, III is the region of amorphous phase separation.

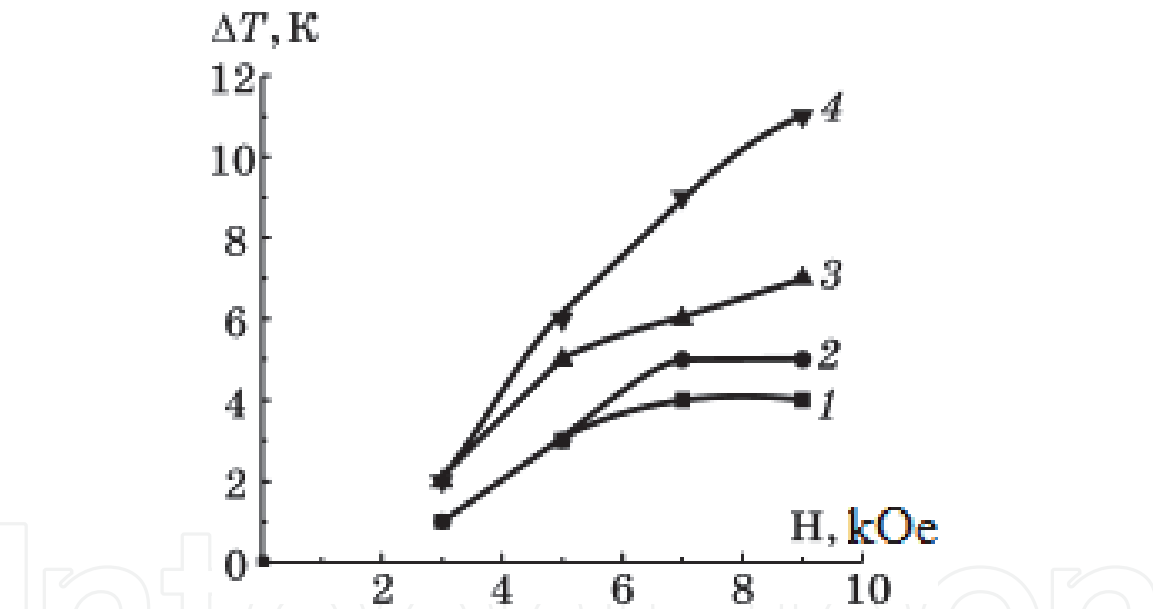


Figure 33.
Dependence ΔT vs. H for the HPC-3-DMAc system: $\omega_2 = 0.46$ (1), 0.48 (2), 0.50 (3), and 0.51 (4).

It should be noted that for the solutions of the lower-molecular-weight sample HPC, the value of ΔT is significantly larger. This proves the better orientation of smaller molecules in the magnetic field, which coincides with the results of the other studies (**Figure 34**) [12].

4.1 Magnetic field energy stored by solutions and temperature of phase transitions

The solutions of cellulose derivatives exhibit the formation of the cholesteric liquid crystals [1]. The exposure of solutions in magnetic field induces the transition of the cholesteric liquid crystal to the forced nematic liquid crystal. And such transition has a threshold character with the critical intensity of the magnetic field $H_{\text{critical}} \sim 10^3$ Oe. For the calculation of energy E stored by a unit of the solution

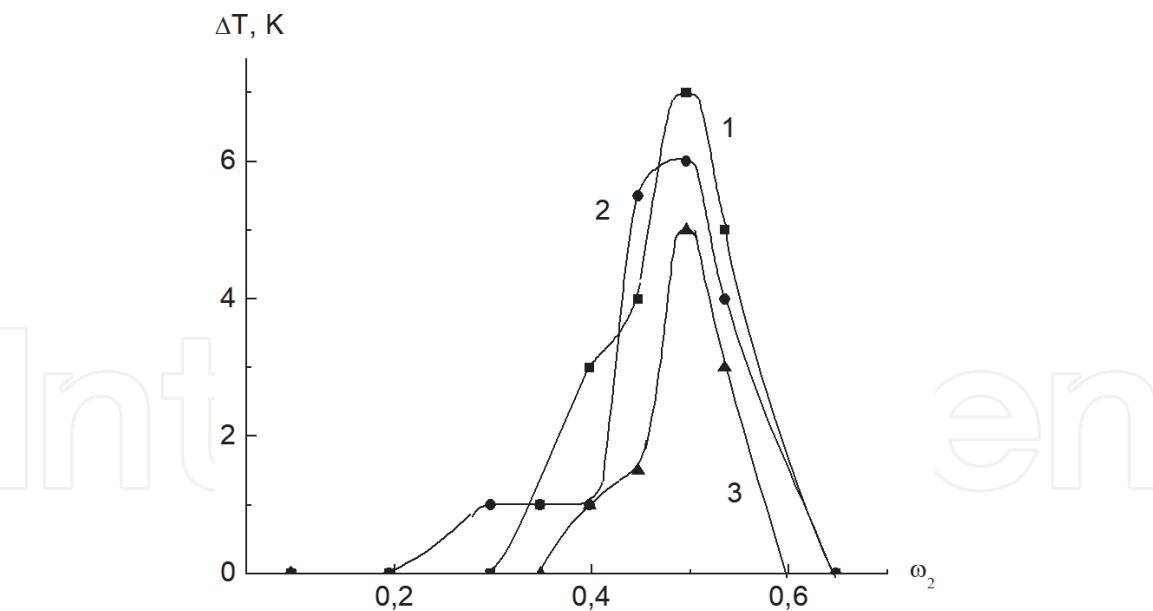


Figure 34.
Concentration dependence of ΔT for the HPC-1-water system: $H = 5$ (1), 9 (2), and 13 kOe (3).

System	$-\chi \cdot 10^7$
HPC-1	18.1
HPC-1-DMAc ($\omega_2 = 0.5$)	6.9
HPC-1-water ($\omega_2 = 0.5$)	3.4
HPC-1-CH ₃ COOH ($\omega_2 = 0.3$)	71.3
CEC	5.3
CEC-DMAc ($\omega_2 = 0.5$)	6.7

Table 6.
Magnetic susceptibility of the systems.

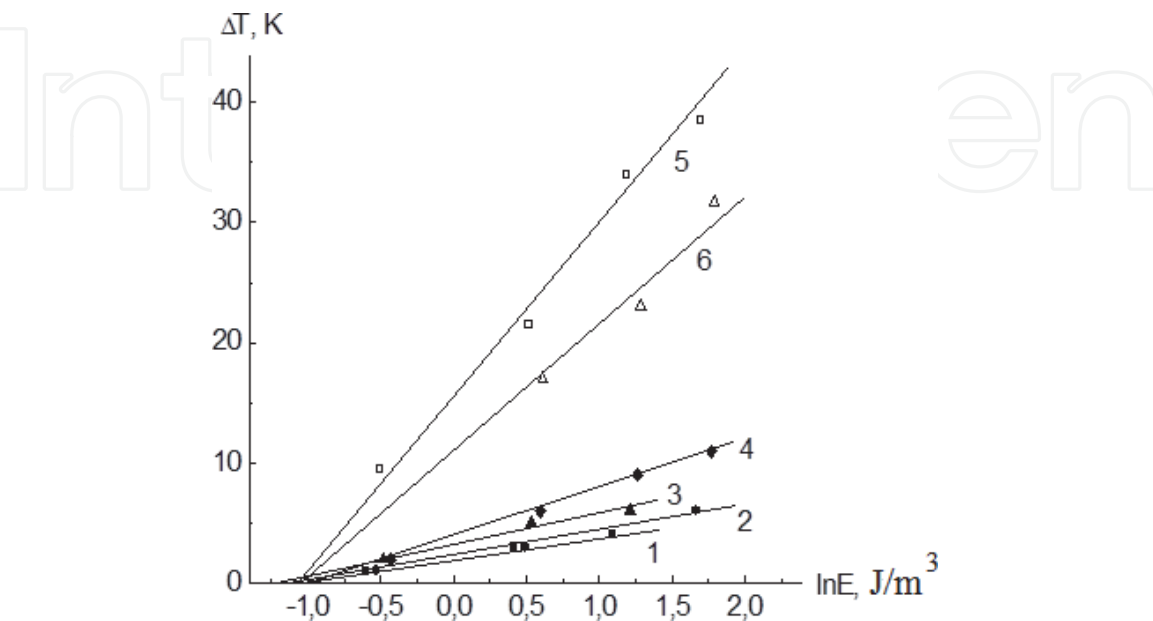


Figure 35.
Plot of ΔT vs. $\ln E$ for the systems: HPC-3-DMAc: $\omega_2 = 0.46$ (1), 0.48 (2), 0.50 (3), and 0.51 (4); HPC-1-DMAc: $\omega_2 = 0.49$ (5), and 0.52 (6).

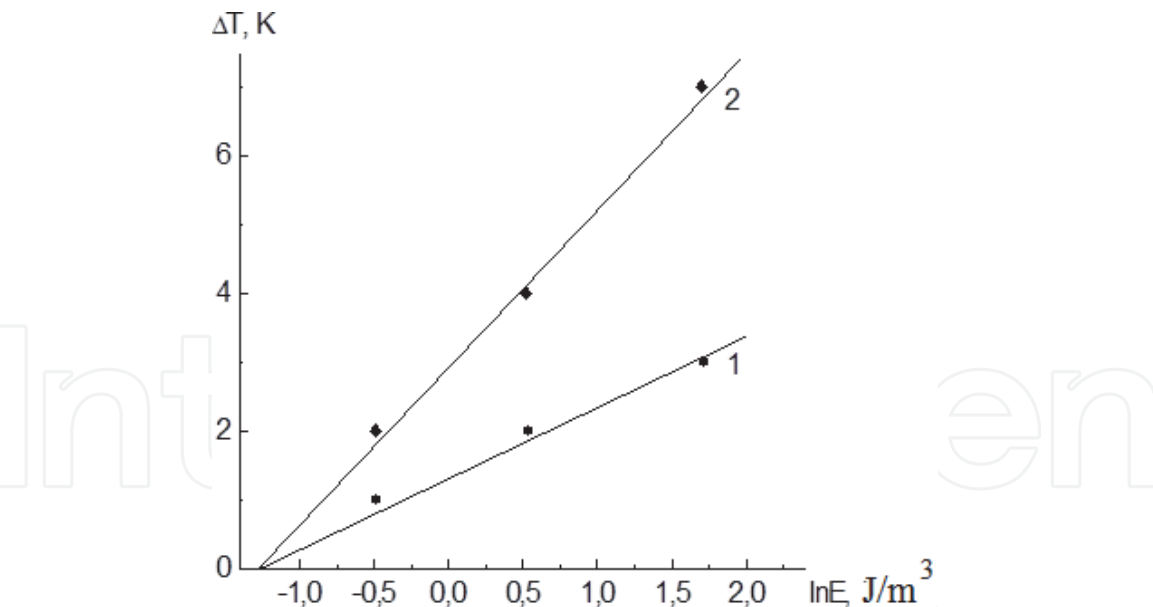


Figure 36.
Plot of ΔT vs. $\ln E$ for CEC-DMAc system: $\omega_2 = 0.46$ (1) and 0.49 (2).

System	$E_0, \text{J/m}^3$	$H_{\text{critical}}, \text{kOe}$
HPC-DMAc	0.34	2.2
CEC-DMAc	0.28	2.0

Table 7.
Calculated values for E_0 and H_{critical} for systems HPC-DMAc, CEC-DMAc.

volume, the values of magnetic susceptibility χ were determined for a number of the systems. **Table 6** lists the results.

All calculated values of χ are negative. Therefore, the studied systems show the diamagnetic properties that agree with their chemical structure. The value of E was calculated according to the equation: $E = -\chi H^2$, where H is the intensity of the magnetic field. It was found that the dependence of ΔT vs. $\ln E$ is described by the straight lines for the systems: HPC-1-DMAc, HPC-3-DMAc, CEC-DMAc, PBG-DMF (**Figures 35 and 36**).

Figure 35 explicitly shows that the smaller the HPC molecules, the better they are oriented in the magnetic field and the higher the ΔT . **Figure 36** also show that the direct dependencies of ΔT on $\ln E$ intersect the abscissa axis virtually at one point, i.e., the temperature change of the LC phase formation in solutions begins from a certain value of the energy E_0 . Thus, the impact of the magnetic field on the phase LC transitions in the solutions of cellulose ethers has a threshold character, i.e., it appears at the magnetic field intensity exceeding the critical value of H_{critical} . The computed values of H_{critical} given in **Table 7** agree with the values given in other studies [1] for H_{critical} of the magnetic field required for the conversion of the cholesteric liquid crystal into a nematic one.

5. Conclusions

The classification of liquid crystals is considered. The phase diagrams of the polymer-solvent systems with liquid crystalline phase separation are described. It has been shown that, as the molecular mass of cellulose ether increases, the boundary curve separating the isotropic region from the anisotropic one on the phase

diagram shifts to the region of higher temperatures and lower concentrations of the polymer. The replacement of the hydroxypropyl radical in cellulose ether units with ethyl or hydroxyethyl radicals leads to a decrease in the concentration of LC phase formation. The introduction of nitro groups into the units of CEC chains increases the rigidity of chains; therefore the degree of asymmetry of macromolecules grows and the LC phase is formed at lower concentrations of the polymer. The higher the polarity of solvent molecules, the more negative the Gibbs energy of mixing and the higher the second virial coefficients, that is, the better the interaction between the components. Thus, in a first approximation, the dipole moment can be used as an estimate of solvent quality for cellulose ethers. The rigid macromolecules orient easily in the external fields. This results in: the type of liquid crystal changes from the cholesteric to the nematic one; the domain structure is formed in the solutions; the concentration dependency of ΔT (ΔT is the difference of T_{ph} in the field and in its absence, respectively) is described by the curve exhibiting maximum. The higher the magnetic field intensity, more evident the effects. The smaller the macromolecules, the more profound are their orientations along the lines of force of magnetic field and the bigger the ΔT value. The ΔT value is determined by the field energy E (E is the energy of a magnetic field, stored by a solution volume unit).


The processes of self-assembly of nanomolecules are most intensive in the solutions of rigid-chain polymers. This process has a “packet” mechanism. In diluted solutions there exist isolated macromolecules, which, within the concentrations of 2–5% (depending on the polymer molecular weight), form supramolecular particles: “packets,” which remain stable (do not change dimensions) in a sufficiently wide range (from 10 to 30%). With a further increase in the polymer concentration, the number of packets (nuclei of the new LC-phase) increases while their sizes are conserved. The system transition to the fully LC state is caused by the aggregation of packets and the formation of large particles.

Author details

Sergey Vshivkov* and Elena Rusinova
Ural Federal University, Ekaterinburg, Russia

*Address all correspondence to: sergey.vshivkov@urfu.ru

IntechOpen

© 2022 The Author(s). Licensee IntechOpen. This chapter is distributed under the terms of the Creative Commons Attribution License (<http://creativecommons.org/licenses/by/3.0>), which permits unrestricted use, distribution, and reproduction in any medium, provided the original work is properly cited. 

References

- [1] Papkov SP, Kulichikhin VG. Liquid Crystalline State of Polymers. Moscow: Chemistry; 1977. 240 p. [in Russian]
- [2] Reinitzer F. Beitrage zur Kenntniss des Cholesterins. Wiener Monatshefte für Chemie. 1888;**9**:421-441
- [3] Lehman O. Über Fliessende Kristalle. Zeitschrift für Physikalische Chemie. 1889;**4**:462-472
- [4] Zhdanov SI, editor. Liquid Crystals. Moscow: Chemistry; 1979. 328 p. [in Russian]
- [5] Sonin AS. Introduction to Liquid Crystal Physics. Moscow: Nature; 1983. 400 p. [in Russian]
- [6] Blyumshteyn A, editor. Liquid Crystalline Order in Polymers. Moscow: Mir; 1981. 302 p. [in Russian]
- [7] Andropov VV, Barmatov EB, Shibaev VP, Philippov AP. Dynamics of orientation of nematic copolymer and its liquid crystal mixtures with low molecular weight additive. Vysokomolekulârnye soedineniâ. Seriâ A. 2002;**44**:1111-1118
- [8] Barmatov EB, Medvedev AV, Ivanov SA, Barmatova MV, Shibaev VP. Phase state and photooptical behavior of mixtures of functionalized liquid crystal copolymers with low molecular weight photochromic additives stabilized by hydrogen bonds. Vysokomolekulârnye soedineniâ. Seriâ A. 2001;**43**:468-477
- [9] Kimura T. Study on the effect of magnetic field on polymeric materials and its application. Polymer Journal. 2003;**35**:823-843. DOI: 10.1295/polymj.35.823
- [10] Moore JS, Stupp SI. Orientation dynamics of main-chain liquid crystal polymers. 2. Structure and kinetics in a magnetic field. Macromolecules. 1987; **20**:282-293. DOI: 10.1021/ma00168a009
- [11] Yamato M, Tsunehisa Kimura T. Magnetic Processing of Diamagnetic Materials. Polymers. 2020;**12**:1491-1514. DOI: 10.3390/polym12071491
- [12] Vshivkov SA. Phase Transitions and Structure of Polymer Systems in External Fields. Newcastle: Cambridge Scholars Publishing; 2019. 370 p
- [13] Vshivkov SA, Rusinova EV. Magnetorheology of polymer systems. In: Rivera-Armenta JL, Salazar Crus BA, editors. Polymer Rheology. London: InTechOpen; 2018. pp. 3-28. DOI: 10.5772/intechopen.75768
- [14] Meuer RB. Distortion of a cholesteric structure by a magnetic field. Applied Physics Letters. 1969;**14**: 208-212. DOI: 10.1063/1.1652780
- [15] de Gennes PG. Calcul de la distorsion d'une structure cholesterique par un champ magnetique. Solid State Communications. 1968;**6**:163-165. DOI: 10.1016/0038-1098(68)90024-0
- [16] DuPre DB, Duke RW. Temperature, concentration, and molecular weight dependence of the twist elastic constant of cholesteric poly- γ -benzyl-L-glutamate. The Journal of Chemical Physics. 1975;**63**:143-148. DOI: 10.1063/1.431066
- [17] Duke RW, DB DP, Hines WA, Samulski ET. Poly(γ -benzyl L-glutamate) helix-coil transition. Pretransition phenomena in the liquid crystal phase. Journal of the American Chemical Society. 1976;**98**:3094-3101
- [18] Miller WG, Wu CC, Wee EL, Santee GL, Rai JH, KD, Goebel KD. Thermodynamics and dynamics of polypeptide liquid crystals. Pure and

Applied Chemistry. 1974;**38**:37-58.
DOI: 10.1351/pac197438010037

[19] Ciambella J, Stanier DC, Rahatekar SS. Magnetic alignment of short carbon fibres in curing composites. *Composites. Part B, Engineering*. 2017;**109**:129-137.
DOI: 10.1016/j.compositesb.2016.10.038

[20] Teranishi S, Kusumi R, Kimura F, Kimura T, Aburaya K, Maeyama M. Biaxial magnetic orientation of zinc citrate as nucleating agent of poly (L-lactic acid). *Chemistry Letters*. 2017; **46**:830-832. DOI: 10.1246/cl.170092

[21] Horii S, Arimoto I, Doi T. Linear drive type of modulated rotating magnetic field for a continuous process of three-dimensional crystal orientation. *Journal of the Ceramic Society of Japan*. 2018;**126**:885-888. DOI: 10.2109/jcersj2.18128

[22] Chung JY, Lee JG, Baek YK, Shin PW, Kim YK. Magnetic field-induced enhancement of thermal conductivities in polymer composites by linear clustering of spherical particles. *Composites. Part B, Engineering*. 2018;**136**:215-221. DOI: 10.1016/j.compositesb.2017.10.033

[23] Vshivkov SA, Avvakumova AS. Effect of magnetic field on the rheological properties of poly(ethylene glycol) and poly(dimethylsiloxane) mixtures with aerosil and iron nanoparticles. *Polymer Science, Series A*. 2017;**59**:764-771. DOI: 10.1134/S0965545X17050170

[24] Vshivkov SA, Zhernov IV, Nadol'skii AL, Mizyov AS. Effect of magnetic field on phase transitions in solutions and melts of flexible polymers. *Polymer Science, Series A*. 2017;**59**: 465-472. DOI: 10.1134/S0965545X17040149

[25] Naga N, Ishikawa G, Noguchi K, Takahashi K, Watanabe K, Yamato M.

Magnetic-field induced alignment of low molecular weight polyethylene. *Polymer (Guildf)*. 2013;**54**:784-790.
DOI: 10.1016/j.polymer.2012.12.016

[26] Vshivkov SA, Rusinova EV, Klyuzhin ES, Kapitanov AA. Effect of magnetic field on phase transitions and structure of polyelectrolyte solutions. *Polymer Science. A*. 2020;**62**:62-69.
DOI: 10.1134/S0965545X19050183

[27] Naga N, Saito Y, Noguchi K, Takahashi K, Watanabe K, Yamato M. Magnetic-field-induced alignment of syndiotactic polystyrene. *Polymer Journal*. 2016;**48**:709-714. DOI: 10.1038/pj.2016.21

[28] Gopinadhan M, Choo Y, Osuji CO. Strong orientational coupling of block copolymer microdomains to smectic layering revealed by magnetic field alignment. *ACS Macro Letters*. 2016;**5**: 292-296. DOI: 10.1021/acsmacrolett.5b00924

[29] Vshivkov SA, Rusinova EV, Kudrevatykh NV, Galyas AG, Alekseeva MS, Kuznetsov DK. Phase transitions of hydroxypropylcellulose liquid-crystalline solutions in magnetic field. *Polymer Science. A*. 2006;**48**: 1115-1119. DOI: 10.1134/S0965545X06100142

[30] Vshivkov SA, Rusinova EV, Kutsenko LI, Galyas AG. Phase transitions in liquid-crystalline cyanoethyl cellulose solutions in magnetic field. *Polymer Science. B*. 2007;**49**:200-202. DOI: 10.1134/S156009040707007X

[31] Vshivkov SA, Rusinova EV. Effect of magnetic fields on phase transitions in solutions of cellulose derivatives. *Polymer Science. A*. 2008; **50**:725-732. DOI: 10.1134/S0965545X08070018

[32] Vshivkov SA, Rusinova EV, Galyas AG. Phase diagrams and

- rheological properties of cellulose ether solutions in magnetic field. *European Polymer Journal*. 2014;**59**:326-332. DOI: 10.1016/j.eurpolymj.2014.07.042
- [33] Vshivkov SA, Rusinova EV, Galyas AG. Effect of a magnetic field on the rheological properties of the rheological properties of cellulose ether solutions. *Polymer Science. A*. 2012;**54**: 827-832. DOI: 10.1134/S0965545X1211003X
- [34] Vshivkov SA, Rusinova EV, Galyas AG. Relaxation character of the rheological behavior of cellulose ether solutions in a magnetic field. *Russian Journal of Applied Chemistry*. 2014;**87**: 1140-1145. DOI: 10.1134/S1070427214080217
- [35] Vshivkov SA, Soliman TS. Effect of a magnetic field on the rheological properties of the systems hydroxypropyl cellulose – ethanol and hydroxypropyl cellulose – dimethyl sulfoxide. *Polymer Science. A*. 2016;**58**: 307-314. DOI: 10.1134/S0965545X16030184
- [36] Vshivkov SA, Soliman TS. Phase transitions, structures, and rheological properties of hydroxypropyl cellulose—ethylene glycol and ethyl cellulose—dimethylformamide systems in the presence and in the absence of a magnetic field. *Polymer Science. A*. 2016;**58**:499-505. DOI: 10.1134/S0965545X16040143
- [37] Plate NA, editor. *Liquid-crystalline polymers*. Moscow: Chemistry; 1988. 416 p. [in Russian]
- [38] Onsager L. The effect of shape on the interaction of colloidal particles. *Annals of the New York Academy of Sciences*. 1949;**51**:627-659
- [39] Flory PJ. Phase equilibria in solutions of rod-like particles. *Proceedings of the Royal Society of London A*. 1956;**234**:73-89
- [40] Miller WG, Wu CC, Wee EL, Santee GL, Rai JH, Gaebel KG. Thermodynamics and dynamics of polypeptide liquid crystals. *Pure and Applied Chemistry*. 1974;**38**:37-54. DOI: 10.1351/pac197438010037
- [41] Iovleva MM, Papkov SP, Mil'kova LP, Kalmykova VD, Volokhina AV, Kudryavtsev GI. Temperature-concentration boundaries of liquid crystalline state of poly-p-benzamide. *Polymer Science. U.S.S.R. B*. 1976;**18**:830-832
- [42] Papkov SP, Kulichikhin VG, Kalmykova VD, Malkin AY. *Journal of Polymer Science Polymer Physics Edition*. 1974;**12**:1753-1770
- [43] Sasaki S, Tokuma K, Uematsu I. Phase behavior of poly(γ -benzyl L-glutamate) solutions in benzyl alcohol. *Polymer Bulletin*. 1983;**10**:539-546. DOI: 10.1007/BF00285373
- [44] Nakajima A, Hirai T, Hayashi T. Phase relationship of rodlike polymer, poly(p-phenyleneterephthalamide) in sulfuric acid-water system. *Polymer Bulletin*. 1978;**1**:143-147. DOI: 10.1007/BF00255729
- [45] Kiss G, Porter RS. Rheology of the concentrated solutions of poly- γ -benzyl-L-glutamate. *American Chemical Society, Polymer Preprints*. 1977;**18**: 185-186
- [46] Lukashova NV, Volokhina AV, Papkov SP. Phase conversions and viscosity properties of aromatic copolyamide solutions. *Vysokomolekulârnye Soedineniâ. Seriâ B*. 1978;**20**:151-154
- [47] Konevets VI, Andreeva VM, Tager AA, Ershova IA, Kolesnikova EN. Studying of the moderate-concentrated solution structure of some polyamides in the composition region, preceding the liquid crystal formation.

Vysokomolekulárnye soedineniâ.
Seriâ A. 1985;27:959-967

[48] Kulichikhin VG, Golova LK. Liquid-crystalline state of cellulose and cellulose derivatives. *Khim Drev.* 1985;3: 9-27

[49] Zugenmaier P, Vogt U. Structural investigations on cellulose tricarbanilate: Conformation and liquid crystalline behavior. *Macromolekulare Chemie.* 1983;194:1749-1760.
DOI: 10.1002/macp.1983.021840818

[50] Werbowyj RS, Gray DG. Ordered phase formation in concentrated hydroxypropylcellulose solutions. *Macromolecules.* 1980;13:69-73

[51] Conio G, Bianchi E, Ciferri A, Tealdi A, Aden MA. Mesophase formation and chain rigidity in cellulose and derivatives: 1. (Hydroxypropyl) cellulose in dimethylacetamide. *Macromolecules.* 1983;16:1264-1270

[52] Vshivkov SA, Rusinova EV. Effect of component nature on liquid – crystalline transitions in solutions of cellulose ethers. *Polymer Science. A.* 2018;60:65-73. DOI: 10.1134/S0965545X18010078

[53] Vshivkov SA, Galyas AG, Kutsenko LI, Tyukova IS, Terziyan TV, Shepetun AV. Self-organization of macromolecules and liquid-crystalline phase transitions in solutions of cellulose ethers. *Polymer Science. A.* 2011;53:1-5. DOI: 10.1134/S0965545X1101010X

[54] Vshivkov SA, Galyas AG. Mechanism of self-assembly of rigid–chain macromolecules of cellulose ethers in solutions. *Polymer Science. A.* 2011;53:1032-1039. DOI: 10.1134/S0965545X1100130

[55] Vshivkov SA, Adamova LV, Lirova BI. Thermodynamic parameters of the interaction of cellulose ethers

with low-molecular-mass liquids. *Polymer Science. A.* 2012;54:821-826.
DOI: 10.1134/S0965545X12080123

[56] Shimamura K, White JL, Feller JF. Hydroxypropylcellulose, a thermotropic liquid crystal: Characteristics and structure development in continuous extrusion and melt spinning. *Journal of Applied Polymer Science.* 1981;26: 2165-2180. DOI: 10.1002/app.1981.070260705

[57] Charlet G, Gray DG. Solid cholesteric films cast from aqueous (hydroxypropyl)cellulose. *Macromolecules.* 1987;20:33-38.
DOI: 10.1021/ma00167a007

[58] Fischer H, Murray M, Keller A, Odell JA. On the phase diagram of the system hydroxypropylcellulose-water. *Journal of Materials Science.* 1995;30: 4623-4627. DOI: 10.1007/BF01153071

[59] Belousov VP, Panov MY. Thermodynamics of Nonelectrolyte Aqueous Solutions. Leningrad: Khimiya; 1983. 264 p. [in Russian]

[60] Vshivkov SA, Adamova LV, Rusinova EV, Safronov AP, Dreval VE, Galyas AG. Thermodynamics of liquid-crystalline solutions of hydroxypropyl cellulose in water and ethanol. *Polymer Science. A.* 2007;49:578-583.
DOI: 10.1134/S0965545X07050124

[61] Fortin S, Charlet G. Phase diagram of aqueous solutions of (hydroxypropyl) cellulose. *Macromolecules.* 1989;22: 2286-2292. DOI: 10.1021/ma00195a050

[62] Kamide K, Saito M, Abe T. Dilute solution properties of water-soluble incompletely substituted cellulose acetate. *Polymer Journal.* 1981;13: 421-431. DOI: 10.1295/polymj.13.421

[63] Ravdel AA, Ponomareva AM. Short Handbook of Physicochemical Values. Leningrad: Chemistry. 232 p

[64] Tager AA. Foundations of Nonelectrolyte Solutions Science. Yekaterinburg: Ural. Gos. University; 1993. 312 p. [in Russian]

[65] Heller W, Bhathagar HL, Nakagaki M. Theoretical investigations on the light scattering of spheres. XIII. The “wavelength exponent” of differential turbidity spectra. The Journal of Chemical Physics. 1962;**36**: 1163-1170. DOI: 10.1063/1.1732710

[66] Heller W, Pangonis WL. Theoretical investigations on the light scattering of colloidal spheres. I. The specific turbidity. The Journal of Chemical Physics. 1957;**26**:498-505. DOI: 10.1063/1.1743332

[67] Heller W. Theoretical investigations on the light scattering of spheres. XV. The wavelength exponents at small α values. The Journal of Chemical Physics. 1964;**40**:2700-2704. DOI: 10.1063/1.1725583

[68] Klenin VI, Shchegolev SY, Lavrushin VL. Characteristic Functions of Light Scattering from Disperse Systems. Saratov: Saratovsk. Gos. University; 1977. 177 p. [in Russian]

[69] Schulz L, Seger B, Buchard W. Structures of cellulose in solution. Macromolecular Chemistry and Physics. 2000;**201**:2008-2022. DOI: 10.1002/1521-3935(20001001)201:15<2008::AID-MACP2008>3.0.CO;2-H

[70] Kuhn W, Moser P. Einfluss der Bildung loser Molekulaggregate auf die Viskosität der Lösungen macromolekular Stoffe. Macromolekulare Chemie. 1961; **44-46**:71-77. DOI: 10.1002/macp.1961.020440107